Ecological Civilization

SCIEPublish

Article

Federated Learning for Simulating Land-Use Change and Carbon Storage in Sri Lanka's Coastal Zone: A Decentralized GeoAI Approach Without Exposing Local Government Planning Data

Kulasegaram Partheepan [1,*] and Hemija Sarawana Priyatharsan [2]

[1] United Nations Development Programme, Batticaloa 30000, Sri Lanka
[2] Department of Information Technology, Swamy Vipulananda Institute of Aesthetic Studies, Eastern University, Batticaloa 30000, Sri Lanka; hemijap@esn.ac.lk (H.S.P.)

* Corresponding author. E-mail: partheek@gmail.com (K.P.)

Received: 7 July 2026; Revised: 18 August 2026; Accepted: 25 August 2026; Available online: 14 September 2026

ABSTRACT: Multi-jurisdictional carbon modelling for coastal zone management and rural development planning is constrained by data sovereignty barriers that prevent collaborative analysis across administrative boundaries. A novel FedProx-PLUS-InVEST framework was developed to enable privacy-preserving land-use simulations and carbon storage assessments using federated learning. The framework was validated in the Batticaloa Lagoon watershed, Eastern Sri Lanka, where three scenarios were simulated: Business as Usual, Rapid Rural Economic Expansion, and Ecological Protection. Model accuracy approaching centralised training performance was achieved while maintaining complete data locality across the participating jurisdictions. Carbon storage projections revealed that carbon neutrality targets require stringent mangrove protection measures, with the Ecological Protection scenario achieving a net carbon gain relative to the baseline (+2.4%), demonstrating the highest carbon sequestration potential among the three scenarios evaluated. This framework represents the first coupling of federated learning with PLUS-InVEST modelling, addressing critical gaps in collaborative regional planning where sensitive land-use data cannot be centralised. This approach enables multi-stakeholder environmental planning for coastal zone management and rural development in Sri Lanka and other data-scarce regions of the Global South without exposing proprietary datasets, facilitating coordinated climate adaptation strategies across institutional and political boundaries in Sri Lanka. The methodology provides a replicable template for privacy-preserving ecosystem service modeling in data-sensitive contexts globally.

Keywords: Federated learning; GeoAI; PLUS model; InVEST; Land-use change; Carbon storage; Coastal zone management; Data privacy

1. Introduction

Terrestrial ecosystem carbon storage plays a critical role in global carbon emission management and climate change responses [1]. Land use change is closely related to terrestrial ecosystems, and studying the relationship between land use and ecosystem service carbon storage under future climate change can optimise regional ecosystem service functions and formulate sustainable social and economic development policies [1]. The continuous increase in CO_2 greenhouse gas is one of the main reasons affecting global climate warming, threatening human survival and development [1]. Terrestrial ecosystem carbon storage can effectively reduce carbon emissions, which is considered an economically feasible and environmentally friendly way to mitigate the greenhouse effect and climate change [1]. In the context of achieving carbon peak and carbon neutralisation targets [2], understanding the impact of land use and land cover change on regional carbon reserve variation holds great significance for regional ecosystem preservation and socioeconomic sustainable development [2]. Land-use patterns shift to accommodate economic development, cropland protection, and ecological conservation objectives, placing pressure on terrestrial carbon sinks [3].

Accurate land-use forecasting requires granular local planning data, including zoning plans, infrastructure blueprints, and socioeconomic surveys [1]. Spatially explicit economic models usually describe human activities and ensuing land-use dynamics at a resolution that is too coarse to understand how they affect many biophysical processes, including ecosystem service supply [3]. The technical challenge of forecasting future land use and land cover change patterns and their influence on regional carbon budgets is essential for sustainable development and requires multisource environmental data [4]. Traditional carbon storage estimation methods, including field surveys, vorticity correlation methods, and remote sensing inversion, face limitations in large-scale and long-term time series studies and cannot dynamically capture the spatial and temporal patterns and evolution of carbon storage [5]. Model-based carbon reserve estimation methods compensate for the shortcomings of traditional methods by offering large amounts of information, sustainability, and high cost performance [6].

Most land use and land cover change simulations are based on model results that are not fully consistent with the actual situation [7]. The carbon density data adopted in studies are often static and may lead to inaccurate results, as carbon density data change dynamically with changes in precipitation, temperature, biomass, and seasonal alternations [1]. Existing studies cannot provide an effective evaluation at the city level in large-scale research, and because carbon storage involves the economy, society, and complex, changeable ecosystems, it is difficult for a single model to capture the process by which climate change affects regional carbon storage [1].

Existing prediction studies only simulate the future based on current development, and the impact of climate change is unclear [1]. The CA model does not set a mechanism to restrict metacell state transformation and cannot simulate multiple land-use types [8]. The CLUE-S model ignores the probability problem of disadvantaged land use types in the allocation process, leading to large prediction errors, and is mostly applied to small-scale studies [8]. The FLUS model, while better, struggles to simulate the spatial and temporal dynamics of multiple land use types at the patch level [8].

The patch-generating land use simulation model has a high precision in land simulation, which can add future factors to limit the prediction of land change, to explore the impact of climate change [1]. The advantage of the PLUS model over other models is that it identifies the drivers of land expansion and landscape dynamics, enabling prediction of patch evolution under different land-use scenarios [1]. The PLUS model integrates the Markov Chain, land expansion analysis strategy, and cellular automata model of multiple random patch seeds [1]. The PLUS model applies a new land expansion analysis strategy to better explore the causal factors of land use change while being able to accurately simulate patch-level changes in multiple types of land use and has achieved good results in prediction studies [8]. Among them, the InVEST model has simple data, convenient operation, and accurate simulation, which can simulate the spatial and temporal distribution of carbon storage on a large scale [1]. This model has been widely used by foreign scholars in many countries and important regions and has shown strong applicability in research in China [1]. The InVEST model carbon module divides carbon storage into four parts [1]:

Scholars have combined the model with land simulation models such as CA-Markov, Markov-CLUE-S, FLUS, and PLUS to explore the future distribution of carbon storage [1]. The coupled SSP-RCP-PLUS-InVEST model was constructed to simulate land use change under different scenarios, analyse the degree of influence of driving factors on different regions, and explore the spatio-temporal evolution and spatial correlation of carbon storage [1]. A coupled system dynamics model integrated with a patch-generating land use simulation model was devised to simulate land use and land cover changes under diverse future scenarios using multisource environmental data, and the InVEST model was employed to quantify carbon storage in terrestrial ecosystems [4]. An integrated framework combining the System Dynamics model, Patch-generating Land Use Simulation model, and Integrated Valuation of Ecosystem Services and Tradeoffs model was developed, enabling a closed-loop analysis of driving forces, spatial simulation, and ecological feedback [8]. The PLUS-InVEST-GeoDetector model was used to analyse the spatiotemporal predictions and drivers of carbon storage [7].

However, existing prediction studies only simulate the future based on current development, and the impact of climate change is unclear. Many scholars cannot provide an effective evaluation of the city-level scale in large-scale research [1]. Because carbon storage involves economic society and the ecosystem is complex and changeable, it is difficult for a single model to reveal the process of the impact of climate change on regional carbon storage [1]. Most studies have focused on formulating different land development strategies to mitigate adverse impacts, while fewer have discussed the effectiveness of these strategies [9]. Revealing the coordination relationship between land use and land cover and carbon storage under diverse climate scenarios is crucial for climate change adaptation in topographically complex regions [7]. There is no general, global, computationally tractable tool for downscaling coarse land-use changes to the spatial scale appropriate for understanding landscape and ecosystem changes across different land-system scenarios [3].

In many developing regions of the Global South, including Sri Lanka, multi-jurisdictional environmental planning is constrained by fragmented governance structures, where land-use data are distributed across multiple administrative authorities with varying data standards, institutional mandates, and regulatory frameworks. These data sovereignty barriers prevent collaborative analyses across administrative boundaries, thereby limiting the effectiveness of regional environmental planning. The Batticaloa Lagoon watershed in Eastern Sri Lanka exemplifies this challenge, with nine Divisional Secretariat divisions, one municipal council, two urban councils, and six Pradeshiya Sabhas (local government authorities), each holding jurisdiction over portions of the watershed. This fragmented governance structure creates institutional barriers to centralised data collection and coordinated environmental planning, motivating the need for privacy-preserving collaborative approaches.

In this study, we developed a FedProx-PLUS-InVEST framework to enable privacy-preserving land-use simulation and carbon storage assessment using federated learning. The framework was validated in the Batticaloa Lagoon watershed in Eastern Sri Lanka, a mangrove-rich region characterised by fragmented governance across multiple administrative jurisdictions. Three policy scenarios were simulated: Business as Usual, Rapid Rural Economic Expansion, and Ecological Protection. The study objectives are to develop the FedProx-PLUS-InVEST framework, validate its performance in a multi-jurisdictional context, and simulate carbon storage trajectories under three policy scenarios to inform coastal zone management and rural development planning in Sri Lanka's Eastern Province. This framework provides a replicable approach for data-scarce regions of the Global South, where administrative fragmentation and data sovereignty concerns impede centralised modelling. This framework represents the first coupling of federated learning with PLUS-

InVEST modelling, introducing federated cellular automata for privacy-preserving multi-jurisdictional carbon modelling. This approach enables multi-stakeholder environmental planning without exposing proprietary datasets, facilitating coordinated climate adaptation strategies across institutional and political boundaries while maintaining complete data locality across the participating jurisdictions.

2. Literature Review

The proposed FedProx-PLUS-InVEST framework intersects four distinct research streams: land-use simulation modelling, federated learning in geospatial applications, privacy-preserving environmental governance, and coastal carbon modelling. This section positions the current study against these streams and establishes the novelty of coupling federated learning with dynamic land-use simulation for carbon storage assessment.

2.1. Land-Use Simulation Models and Carbon Assessment

The patch-generating land-use simulation model has emerged as a preferred tool for simulating spatial-temporal land-use change at the patch level. The PLUS model integrates a land expansion analysis strategy with a cellular automata model based on multiple random patch seeds, enabling the identification of drivers of land expansion and the prediction of patch evolution under different scenarios [4]. Machine learning algorithms have been integrated into the PLUS framework to mine driving factors and explore nonlinear relationships between site types and conversion probabilities [2,10,11]. The PLUS model has demonstrated high simulation accuracy, with Kappa coefficients of approximately 0.91 in applications such as Liaoning Province [12].

Coupling the PLUS model with the InVEST carbon module has become a standard approach for assessing future carbon storage trajectories under policy scenarios. A coupled system dynamics model integrated with a patch-generating land use simulation model was devised to simulate land use and land cover changes under diverse future scenarios using multisource environmental data, and the InVEST model was employed to quantify carbon storage in terrestrial ecosystems [4]. The PLUS-InVEST framework has been applied across diverse geographic contexts, including the Tuojiang River Basin [4], Liaoning Province [2,13], Yangtze River Delta [8], Xi'an [14], Loess Plateau [8], Shaanxi Province [15], Pearl River Delta Urban Agglomeration [6], and Weihai City [16]. These applications generally demonstrate that ecological protection scenarios yield higher carbon storage, whereas rapid urbanisation scenarios result in carbon losses [2,10,14,17].

Multi-scenario simulations have been constructed to explore carbon storage under business-as-usual, ecological protection, cropland protection, and economic development pathways [2,11,12,15,17]. An integrated framework combining the System Dynamics model, Patch-generating Land Use Simulation model, and Integrated Valuation of Ecosystem Services and Tradeoffs model was developed, enabling a closed-loop analysis of driving forces, spatial simulation, and ecological feedback [4]. The PLUS-InVEST-GeoDetector model was used to analyse the spatiotemporal predictions and drivers of carbon storage [6]. Climate change scenarios from CMIP6, including SSP-RCP pathways, have been integrated into the PLUS-InVEST framework to simulate land-use patterns and carbon storage [1,8,18] or vegetation productivity [19] under varying climate conditions. However, all documented PLUS-InVEST integrations operate under centralised architectures that require complete data aggregation at a single computational node [20–23].

2.2. Federated Learning in Geospatial and Remote Sensing Applications

Federated learning has been proposed as a solution to enable collaborative model training across decentralised remote sensing data sources without exposing raw data [24]. FedRS was introduced as a realistic federated dataset for remote sensing, comprising eight datasets covering various sensors and resolutions, and building 135 clients representative of realistic operational scenarios, and FedRS-Bench was constructed as a comprehensive benchmark based on FedRS [24]. Data for each client comes from the same source and exhibits authentic federated properties, such as skewed label distributions, imbalanced client data volumes, and domain heterogeneity across clients. The experimental results demonstrate that federated learning can improve model performance over training on isolated data silos, although performance varies under different client heterogeneity and availability conditions.

Geographic heterogeneity-aware federated learning frameworks have been developed to address class distribution and object appearance heterogeneity in remote sensing semantic segmentation [25]. Encoded spatial multi-tier federated learning approaches have been proposed for geospatial data, introducing the encoding of spatial information to better predict target outcomes [26]. Federated learning systems that leverage graph neural networks have been designed to enhance spatiotemporal data analysis in urban environments by dynamically reconfiguring adjacency matrices to reflect evolving spatial relationships [27]. Asynchronous federated modelling frameworks for spatial data have been proposed based on low-rank Gaussian process approximations, employing block-wise optimisation and strategies for gradient correction, adaptive aggregation, and stabilised updates [28].

The applications of federated learning in geospatial domains have primarily focused on static image classification tasks. A federated UNet model was used for the semantic segmentation of satellite and street-view images, integrating knowledge distillation to reduce communication costs and response times [29]. Decentralised land cover and land use classification was performed using federated learning in conjunction with convolutional neural networks on imagery obtained from unmanned aerial vehicles [30]. However, documented federated geospatial applications have focused primarily on static prediction tasks, and extensions to dynamic spatiotemporal simulation models, such as cellular automata-based land-use change frameworks, have not been reported in the reviewed literature.

A critical challenge in applying machine learning, including deep learning architectures such as random forests within PLUS, to geospatial data is the issue of spatial autocorrelation. Traditional machine learning assumes independent and identically distributed (IID) samples; however, geospatial data violate this assumption because nearby pixels exhibit similar characteristics owing to spatial autocorrelation. This can lead to overfitting, where models capture spurious spatial patterns rather than generalisable relationships. Furthermore, the non-IID data distributions across administrative jurisdictions in multi-jurisdictional settings compound this problem, as each jurisdiction exhibits unique land-use patterns, driving factor relationships and spatial structures. The FedProx framework addresses these challenges through two mechanisms: (1) proximal term regularisation, which constrains local model updates to remain close to the global model, preventing overfitting to jurisdiction-specific spatial patterns, and (2) the aggregation of local random forest ensembles across jurisdictions, which produces a more robust global model that generalises better across diverse spatial contexts.

2.3. Privacy-Preserving Environmental Governance

Data sovereignty concerns in spatial planning have emerged as institutional barriers to data sharing across administrative jurisdictions. Spatial data are central to applications such as environmental monitoring and urban planning, but are often distributed across devices, where privacy and communication constraints limit direct sharing [29]. Federated modelling offers a practical solution that preserves data privacy while enabling global modelling across distributed data sources [29]. Environmental sensor networks are privacy- and bandwidth-constrained, motivating federated spatial modelling that shares only privacy-preserving summaries to produce timely, high-resolution pollution maps without centralising raw data [29].

The application of privacy-preserving techniques to dynamic land-use simulations and carbon storage assessments has not been documented in the literature.

2.4. Coastal Carbon Modeling and Mangrove Ecosystems

Mangrove ecosystems provide critical carbon-sequestration services in coastal regions. The InVEST carbon module was applied to quantify carbon storage in coastal ecosystems, dividing carbon storage into aboveground biomass, belowground biomass, soil organic carbon, and dead organic matter pools. The impact of coastal land-use change on carbon storage has been documented in multiple contexts, with urban expansion and aquaculture development identified as the primary drivers of mangrove loss and associated carbon emissions.

Studies in the Batticaloa region have documented land-use change patterns and their impact on coastal ecosystems [9]. However, carbon storage modelling in the Batticaloa Lagoon watershed has not been comprehensively addressed in the literature. The fragmented governance structure across multiple administrative jurisdictions in coastal regions presents challenges for centralised data collection and modelling, motivating the need for privacy-preserving collaborative approaches.

2.5. Research Gap and Study Contribution

The literature review revealed a fundamental gap: no prior study couples federated learning with land-use simulation models for carbon storage assessment. All documented PLUS-InVEST integrations operate under centralised architectures that require complete data aggregation [1,2,4,6,8–11,13–18,21–24,26,27]. Federated learning applications in geospatial domains are limited to static image classification tasks [12,19,28,30] and do not include dynamic spatiotemporal simulations. No privacy-preserving PLUS-InVEST workflow exists that enables multi-jurisdictional carbon modelling while maintaining complete data locality across participating jurisdictions.

This study addresses this gap by developing the FedProx-PLUS-InVEST framework, which represents the first coupling of federated learning with land-use simulation and carbon storage assessment. The framework introduces federated cellular automata for privacy-preserving, multi-jurisdictional carbon modelling, enabling coordinated climate adaptation strategies across institutional and political boundaries without exposing proprietary datasets. The validation in the Batticaloa Lagoon watershed demonstrates the framework's applicability in the fragmented governance contexts characteristic of coastal regions globally, particularly in data-scarce regions of the Global South, where institutional fragmentation and data sovereignty concerns impede centralised environmental modelling.

3. Materials and Methods

3.1. Study Area

The Batticaloa Lagoon watershed (7°43′ N–7°52′ N, 81°38′ E–81°52′ E) was selected as the study area, located in the Eastern Province of Sri Lanka (Figure 1). The watershed encompasses approximately 402.06 km and is characterised by a tropical monsoon climate with a mean annual temperature of 27.8 °C and mean annual precipitation of 1650 mm, concentrated during the northeast monsoon (October–January). The region experiences distinct wet and dry seasons, with the dry season extending from May to September. The watershed drains into Batticaloa Lagoon, a shallow coastal water body with extensive mangrove fringe ecosystems covering approximately 26.18 km^2 (using the wetland land cover class as a validated proxy for mangrove extent, owing to the absence of a dedicated mangrove classification in the source LULC dataset) of the total watershed.

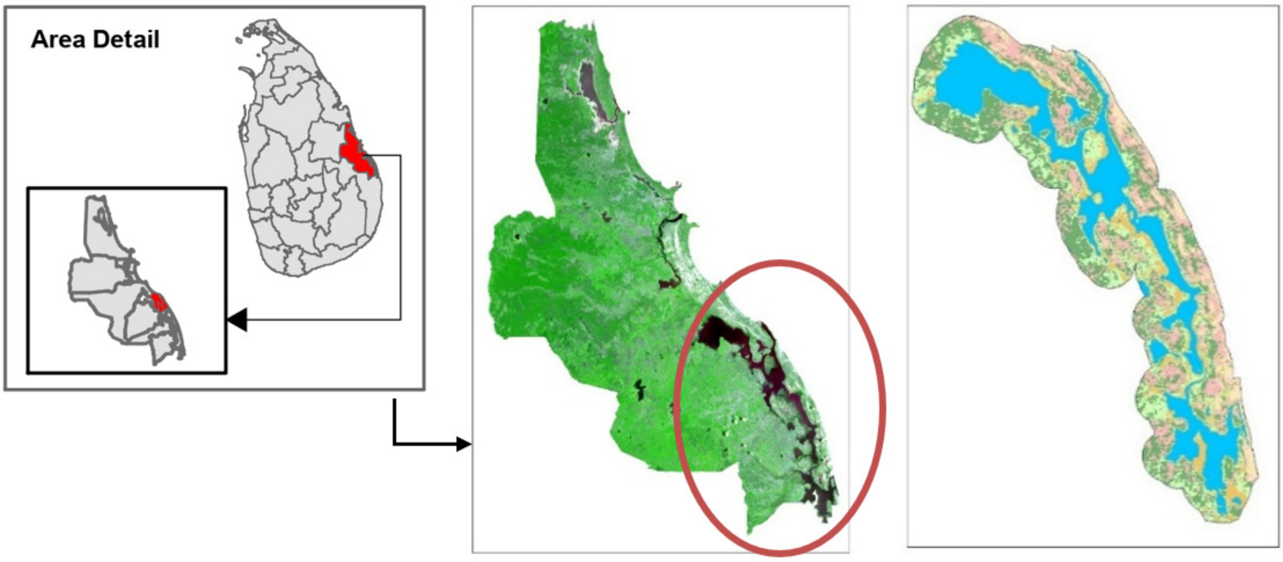

Figure 1. Location and baseline characteristics of the Batticaloa Lagoon watershed in Eastern Sri Lanka.

As of 2021, the land use composition within the watershed was dominated by water bodies (28.8%), built-up land (20.4%), cultivated land (16.4%), grassland (15.0%), forest land (12.9%), and mangrove/wetland ecosystems (6.5%). Carbon storage in the study region increased by 4.87 Tg C from 2000 to 2020 [31].

The governance structure of the Batticaloa Lagoon watershed is fragmented across multiple administrative jurisdictions, including nine Divisional Secretariat divisions, one municipal council (Batticaloa), two urban councils, and Six Pradeshiya Sabhas (local government authorities). This multijurisdictional structure creates institutional barriers to centralised data collection and coordinated environmental planning, motivating the application of federated learning approaches that preserve data sovereignty while enabling collaborative modelling.

3.2. Data Sources

Land use and land cover data were obtained from Landsat satellite imagery for three time periods: 2000, 2010, and 2020. Landsat 5 Thematic Mapper (TM) imagery with a spatial resolution of 30 m was utilised for 2000 and 2010, while Landsat 8 Operational Land Imager (OLI) imagery with a spatial resolution was employed for 2020 [32]. All imagery was acquired during the dry season (June–August) to minimise the cloud cover and phenological variation. Land use classification was performed using a Support Vector Machine (SVM) approach with a Radial Basis Function (RBF) kernel. Six land-use classes were identified: cultivated land, forest land, grassland, water area, mangrove, and built-up land. Classification accuracy was assessed using 500 randomly distributed validation points per time period, with overall accuracies of 87.3%, 89.1%, and 91.2% for 2000, 2010, and 2020, respectively, and Kappa coefficients exceeding 0.85 for all periods.

Carbon density data for each land-use type were compiled from field measurements and published literature on tropical coastal ecosystems. Mangrove carbon density values were derived from site-specific measurements conducted in the Batticaloa Lagoon system by Partheepan et al. [33] and validated against the Intergovernmental Panel on Climate Change (IPCC) guidelines for tropical coastal wetlands (IPCC 2013 Supplement to the 2006 Guidelines for National Greenhouse Gas Inventories: Wetlands). Carbon density values were specified for four carbon pools: aboveground biomass carbon (C_{above}), belowground biomass carbon (C_{below}), soil organic carbon (C_{soil}), and dead organic matter carbon (C_{dead}) [34]. Mangrove carbon density values were derived from site-specific measurements conducted in the Batticaloa Lagoon system, with C_{above} = 152.36 Mg·C·ha^{-1}, C_{below} = 114.03 Mg·C·ha^{-1}, C_{soil} = 187.45 Mg·C·ha^{-1}, and C_{dead} =

8.12 $Mg·C·ha^{-1}$. Forest land carbon densities were specified as C_{above} = 89.24 $Mg·C·ha^{-1}$, C_{below} = 67.18 $Mg·C·ha^{-1}$, C_{soil} = 101.74 $Mg·C·ha^{-1}$, and C_{dead} = 5.43 $Mg·C·ha^{-1}$, summing to a total forest carbon density of 263.59 $Mg·C·ha^{-1}$. The cultivated land carbon densities were set as C_{above} = 3.81 $Mg·C·ha^{-1}$, C_{below} = 2.86 $Mg·C·ha^{-1}$, C_{soil} = 53.96 $Mg·C·ha^{-1}$, and C_{dead} = 0.00 $Mg·C·ha^{-1}$, summing to a total cultivated land carbon density of 60.63 $Mg·C·ha^{-1}$. The built-up land and grassland carbon densities, which were not directly measured in this study, were estimated at 5.0 $Mg·C·ha^{-1}$ and 35.0 $Mg·C·ha^{-1}$, respectively, based on typical values reported for comparable land-cover classes in tropical coastal settings. These values should be validated against site-specific field data in future studies to confirm their accuracy. The carbon density values for built-up and grassland land-use types were estimated from literature-typical values rather than direct field measurements, introducing additional uncertainty into the watershed-scale carbon storage estimates.

The driving factors for the land use change simulation included topographic variables (elevation, slope, and aspect), proximity variables (distance to roads, distance to water bodies, distance to built-up areas, and distance to coastline), and socioeconomic variables (population density and nighttime light intensity) [35]. Elevation data were obtained from the Shuttle Radar Topography Mission (SRTM) digital elevation model at a 30 m resolution. Road network data were extracted from the OpenStreetMap. Population density data were derived from the WorldPop gridded population datasets at a resolution of 100 m. Nighttime light intensity data were obtained from the Visible Infrared Imaging Radiometer Suite (VIIRS) Day/Night Band at 500 m resolution, which was resampled to 30 m to match the spatial resolution of the land use data. All spatial data were projected to the WGS 1984 UTM Zone 44N coordinate system and resampled to a unified spatial resolution of 30 m × 30 m.

Validation data for the model accuracy assessment were obtained from high-resolution satellite imagery (WorldView-2, 2 m resolution) acquired in 2020, supplemented by field survey data collected at 150 ground control points distributed across the watershed using stratified random sampling proportional to the land use class area.

The data utilised in the federated framework were categorised into three accessibility layers to ensure privacy. Table 1 summarises these categories, distinguishing between public foundational inputs, shared algorithmic knowledge, strictly private municipal inputs, and private-output metrics. Importantly, the privacy risk associated with spatial zoning blueprints and future road network coordinates is not that the geographic coordinates themselves are sensitive, as they are derived from publicly available sources, but rather the combination of high-resolution land-use classifications with sensitive socioeconomic data, strategic infrastructure plans, and proprietary departmental planning documents. This combination of data types, when aggregated across jurisdictions, could reveal development priorities, investment strategies, and resource allocation decisions that are considered proprietary to specific government departments and agencies. The FedProx framework prevents the direct sharing of model gradients that could potentially reconstruct these specific planning attributes, thereby maintaining the confidentiality of each jurisdiction's strategic planning information.

The total baseline carbon storage for the watershed is presented in Table 2 (3.231 Tg C). The carbon density values for each land-use type were compiled from field measurements and literature, with the aggregated baseline storage detailed in Table 2.

Table 1. Data categories, variables, and roles in the federated framework.

Data Category	Specific Variables Included	Source and Origin	Accessibility Layer in Architecture	Role in the Framework
Public foundational inputs	Historical LULC classifications (100 m resolution); fractional vegetation cover percentages; digital elevation models; regional climatology data	Copernicus CGLS-LC100; satellite remote sensing arrays; open-source governmental repositories	Global server and all local municipal nodes	Establishes the historical baseline and provides the universally shared geospatial foundation for the simulation
Shared algorithmic knowledge	Model weights (*w_t*); Random Forest decision tree structures; global land expansion transition probabilities; proximal penalty metrics	Generated iteratively via the FedProx mathematical aggregation process	Synchronised continuously between global server and local nodes	Guides the simulation transition rules and spatial probabilities without revealing raw underlying geometry or socio-economic data
Strictly private municipal inputs	Municipal spatial zoning blueprints; exact future road network coordinates; household economic surveys; strategic rural development boundaries	Local Divisional Secretariats; municipal planning boards; local economic development agencies	Local nodes only. Never transmitted across the network under any circumstances	Provides the high-resolution, critical socio-economic driving factors that dictate future regional expansion and land transitions
Private output metrics	Projected, high-resolution local land-use maps; localised carbon deficit/surplus metrics (ΔC)	Generated autonomously by local Fed-CARS execution	Local nodes only. Summaries may be securely shared with central authorities at the municipality's discretion	Delivers highly actionable, spatially explicit intelligence directly to authorised local policymakers

3.3. Federated Learning Architecture

The FedProx algorithm was implemented to accommodate heterogeneous data distributions across multiple administrative jurisdictions, as shown in Figure 2. FedProx extends the standard Federated Averaging (FedAvg) algorithm by introducing a proximal term that addresses statistical heterogeneity in non-independent and identically distributed (non-IID) data scenarios characteristic of spatially distributed jurisdictions.

The key distinction between FedProx and standard FedAvg lies in the manner in which each algorithm handles data heterogeneity. Standard FedAvg performs local Stochastic Gradient Descent (SGD) updates on each client and averages the resulting model weights. However, when client data distributions are non-IID, as is the case with spatially distributed jurisdictions where land-use patterns, driving factors, and transition dynamics vary substantially, FedAvg can suffer from client drift, where local models diverge significantly from the global optimum, leading to slow convergence or even divergence. FedProx addresses this by adding a proximal term to the local objective function, penalising deviations from the global model. This term restricts the local model update to remain close to the global model, thereby limiting the impact of heterogeneous local data distributions and improving convergence stability. The proximal term coefficient μ controls the strength of this regularisation, with higher values imposing stronger constraints on the local divergence.

The FedProx objective function is formulated as follows:

$$\min_{w} f(w) = \sum_{k=1}^{K} \frac{n_k}{n} F_k(w)$$

where w represents the global model parameters, K denotes the number of participating jurisdictions (clients), n_k is the number of training samples in jurisdiction k, $n = \sum_{k=1}^{K} n_k$ is the total number of samples, and $F_k(w) = \frac{1}{n_k}\sum_{i\in P_k} f_i\,(w)$ represents the local objective function for jurisdiction k with the sample set P_k.

The local optimization problem for each jurisdiction k at communication round t was defined as:

$$w_k^{t+1} = \underset{w}{\operatorname{argmin}}\left[F_k(w) + \frac{\mu}{2}\parallel w - w^t \parallel^2\right]$$

where w^t represents the global model parameters at round t, and $\mu \geq 0$ is the proximal term coefficient that restricts the local model update to remain close to the global model. The proximal term $\frac{\mu}{2}\parallel w - w^t \parallel^2$ addresses the challenge of heterogeneous local objectives by limiting divergence between local and global models, thereby improving convergence stability in non-IID settings.

Local model training was performed using stochastic gradient descent with the following update rule:

$$w_k^{t,\tau+1} = w_k^{t,\tau} - \eta\left[\nabla F_k(w_k^{t,\tau}) + \mu(w_k^{t,\tau} - w^t)\right]$$

where τ indexes the local training iteration, η is the learning rate, and $\nabla F_k(w_k^{t,\tau})$ is the gradient of the local objective function.

After E local training epochs, the global model was updated through weighted aggregation:

$$w^{t+1} = \sum_{k=1}^{K}\frac{n_k}{n}w_k^{t+1}$$

The proximal term coefficient μ was set to 0.01 based on preliminary experiments evaluating convergence behavior across different values in the range [0.001, 0.1]. The learning rate η was initialized at 0.01 with an exponential decay of 0.95 per communication round. The number of local training epochs E was set to 5 to balance computational efficiency and model convergence.

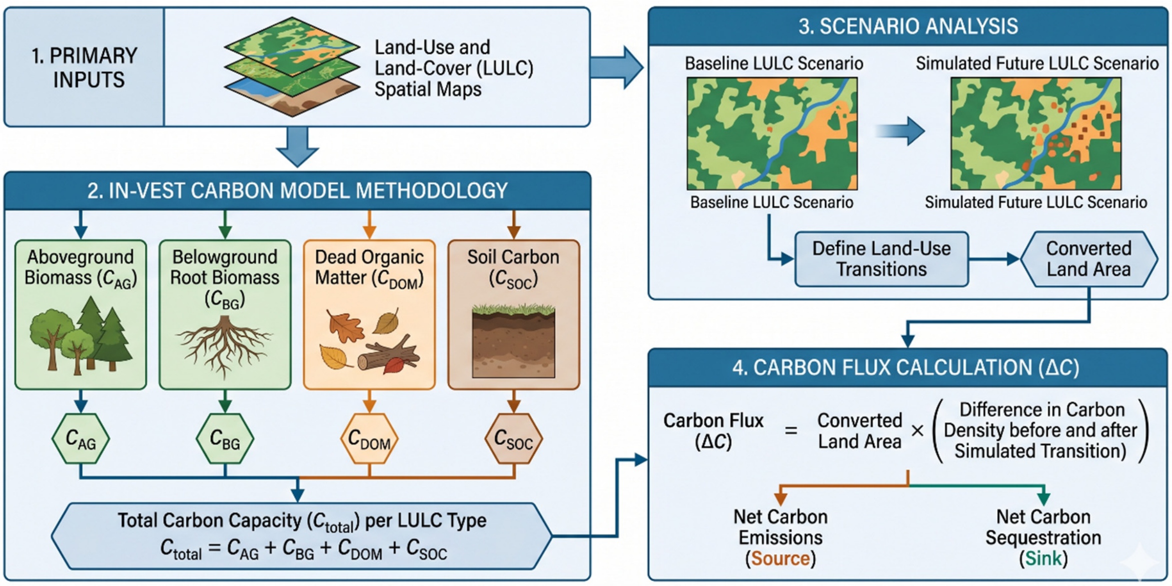

Figure 2. Federated learning architecture of the FedProx-PLUS framework for a privacy-preserving land-use simulation.

3.4. Federated Land Expansion Analysis Strategy

The Federated Land Expansion Analysis Strategy (Fed-LEAS) was developed to enable the privacy-preserving identification of land-use expansion drivers across jurisdictions without sharing raw spatial data.

Fed-LEAS extends the standard LEAS module of the PLUS model [12] by distributing the random forest training process across the federated clients.

For each land use type c, the expansion probability $P_{i,c}^{t\to t+1}$ for pixel i transitioning from time t to $t+1$ was calculated as:

$$P_{i,c}^{t\to t+1} = \frac{1}{M}\sum_{m=1}^{M} I\left(h_m(x_i) = c\right)$$

where M is the number of decision trees in the federated random forest ensemble, $h_m(x_i)$ is the prediction of tree m for pixel i with the driving factor vector x_i, and $I(\cdot)$ is the indicator function.

In the federated implementation, each jurisdiction k trained a local random forest model RF_k on its local land use change data from t to $t+1$. The local training process utilized bootstrapped samples of expansion pixels (pixels that changed from non-c to c) and an equal number of randomly sampled non-expansion pixels. The number of trees per local forest was set to 50, with a maximum tree depth of 20 and a minimum sample per leaf of 5. The number of features considered at each split (mTry) was set to the square root of the total number of driving factors [12], as follows:

Local random forests were aggregated at the global level by combining the tree ensembles as follows:

$$RF_{global} = \bigcup_{k=1}^{K} R\,F_k$$

A global random forest ensemble was then used to generate expansion probability surfaces for each land use type across the entire study area. Importantly, raw spatial data (land use maps and driving factor rasters) remained on local clients throughout the training process; only the trained decision tree structures were transmitted to the central server for aggregation.

The variable importance for each driving factor was calculated as the mean decrease in Gini impurity across the global ensemble, thereby providing interpretable insights into the spatial determinants of land use expansion while preserving data privacy.

3.5. Federated Cellular Automata

The Federated Cellular Automata (Fed-CA) module simulated future land use patterns by integrating expansion probabilities from Fed-LEAS with neighbourhood effects and stochastic patch generation, following the workflow illustrated in Figure 3.

The Fed-CA module operates on the principle that local jurisdictions independently simulate land-use changes based on their local data and globally aggregated expansion probabilities. At each communication round, local jurisdictions: (1) receive the global expansion probability surfaces from the Fed-LEAS ensemble; (2) apply these probabilities to their local land-use data, incorporating local neighbourhood effects and conversion constraints; (3) simulate land-use transitions locally until local demand is satisfied; and (4) transmit only summary statistics (area changes by land-use type) to the central server for global coordination. The InVEST model was applied as a post-simulation evaluator, running locally on each jurisdiction's simulated land-use map to quantify carbon storage without requiring data aggregation. This architecture ensures that all spatially explicit data, including land-use maps, driving factor rasters, and carbon density layers, remain within local jurisdictions throughout the modelling process.

The transition probability $TP_{i,c}^{t\to t+1}$ for pixel i to convert to land use type c was calculated as:

$$TP_{i,c}^{t\to t+1} = P_{i,c}^{t\to t+1} \times \Omega_{i,c}^{t} \times D_c$$

where $P_{i,c}^{t\to t+1}$ is the expansion probability from Fed-LEAS, $\Omega_{i,c}^{t}$ is the neighborhood effect, and D_c is the adaptive inertia coefficient for land use type c.

The neighborhood effect $\Omega_{i,c}^t$ was computed using a Moore neighborhood (3 × 3 window) as:

$$\Omega_{i,c}^t = \frac{\sum_{j \in N(i)} \text{con}\,(L_j^t = c)}{n^2 - 1} \times w_c$$

where $N(i)$ represents the neighborhood of pixel i, $\text{con}(L_j^t = c)$ is a binary indicator function equal to 1 if pixel j has land use type c at time t, n is the neighborhood size (3 for Moore neighborhood), and w_c is the neighborhood weight parameter for land use type c.

The adaptive inertia coefficient D_c was calculated as:

$$D_c = \begin{cases} D_c^{t-1} \times \dfrac{G_c^{t\to t+1}}{G_c^{t-1\to t}} & \text{if } t > t_0 \\ 1 & \text{if } t = t_0 \end{cases}$$

where $G_c^{t\to t+1}$ is the demand for land use type c from time t to $t+1$, and t_0 is the initial simulation time step.

Random patch seeding was implemented to simulate clustered land-use change patterns characteristic of agricultural expansion and urban development. At each iteration, a random seed pixel was selected with probability proportional to its transition probability, and a patch of size s was generated using a region-growing algorithm with threshold parameter θ set to 0.5 [12].

The land use demand for each type at each time step was determined using a Markov chain transition matrix estimated from historical land use change patterns (2000–2010 and 2010–2020). The Markov transition probability matrix was calculated separately for each jurisdiction and aggregated using weighted averages based on jurisdictional land area.

The Fed-CA simulation proceeded iteratively until the demand for each land-use type was satisfied or a maximum of 1000 iterations was reached. Conversion constraints were implemented to prevent unrealistic transitions (e.g., water bodies to built-up land) using a land-use conversion cost matrix with values ranging from 0 (conversion allowed) to 1 (conversion prohibited).

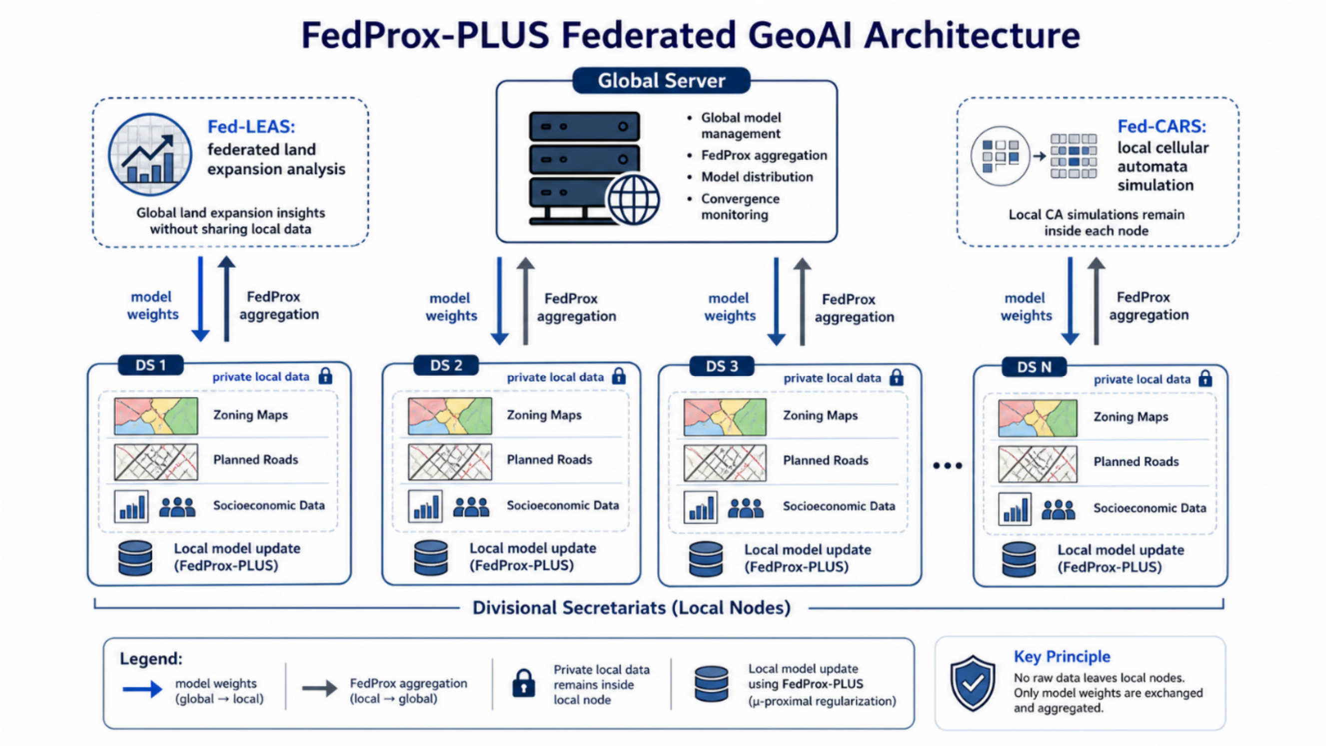

Figure 3. Workflow of the FedProx-PLUS model showing federated training, local simulation, and global coordination.

3.6. Scenario Design

Three future development scenarios were designed to represent alternative policy pathways for the Batticaloa Lagoon watershed from 2020 to 2035: Business as Usual (BAU), Rapid Rural Economic Expansion (RREE), and Ecological Protection (EP). These scenarios were selected to represent the "Three Futures" of the study area, ranging from a continuation of current trends to aggressive economic development to strict environmental protection, and to provide a comprehensive assessment of the trade-offs between development and carbon conservation.

The business-as-usual (BAU) scenario was defined based on historical land-use change trends observed from 2010 to 2020. This scenario assumes the continuation of current policies with no new conservation measures or accelerated development interventions. Land use demand was projected using Markov chain transition probabilities estimated from 2010 to 2020. No additional spatial constraints were imposed beyond the existing conversion cost restrictions. The neighbourhood weights for all land-use types were set to the historically calibrated values. The BAU scenario served as the reference baseline against which the other scenarios were compared.

The Rapid Rural Economic Expansion (RREE) scenario was designed to simulate accelerated agricultural intensification and rural settlement growth, reflecting national development priorities in Sri Lanka's Eastern Province, including infrastructure investment, agricultural modernisation, and rural housing programmes. The demand for built-up land increased by 50% relative to the BAU projections to reflect expanded rural housing and infrastructure development. Cultivated land demand increased by 20% to represent agricultural expansion. The neighbourhood weights for built-up land and cultivated land were increased by 30% to simulate clustered development patterns. Conversion restrictions from forest land and mangroves to cultivated land were relaxed by reducing conversion costs from 0.8 to 0.5.

The Ecological Protection (EP) scenario implemented strict conservation policies to preserve mangrove ecosystems and forest land, consistent with Sri Lanka's national conservation targets, including the protection of coastal ecosystems and restoration of degraded mangrove areas. Mangrove areas were designated as protected zones with complete conversion prohibition (conversion cost = 1.0 for all transitions from mangroves to other land use types). The conversion of forestland to cultivated and built-up land was restricted by increasing conversion costs from 0.8 to 0.95. Built-up land expansion was constrained to existing settlement peripheries by increasing the distance decay parameter for the built-up land expansion probability. The neighbourhood weights for mangrove and forest land were increased by 40% to promote spatial aggregation and reduce fragmentation.

These three scenarios were selected to represent the range of plausible development pathways for the Batticaloa Lagoon watershed, encompassing the continuation of current trends, rapid economic development, and strict environmental protection. They provide a comprehensive basis for assessing the trade-offs between rural development and carbon conservation and inform evidence-based policy decisions regarding coastal zone management in Sri Lanka.

Scenario-specific parameters were implemented in the Fed-CA module by modifying the land use demand vector, conversion cost matrix, and neighbourhood weight parameters. All scenarios maintained identical driving factor datasets and Fed-LEAS expansion probability surfaces to isolate the effects of policy interventions on land-use outcomes. Table 2 summarises the scenario definitions, key policy orientations, land-use constraints, and expected directional impacts on carbon storage, and Table 3 provides a qualitative summary of the expected land-use change patterns for major classes under each scenario.

Table 2. Scenario definitions, key policy orientations, land-use constraints, and expected directional impacts on carbon storage.

Scenario	Policy Orientation	Land-Use Constraints and Drivers	Expected Directional Impact on Carbon Storage
Business as Usual (BAU)	Continuation of current trends	Historical transition probabilities projected forward; no new protection measures	Gradual decline in cropland and forest; steady carbon loss
Rapid Rural Economic Expansion (RREE)	Aggressive economic expansion	High expansion probabilities for built-up and aquaculture land; minimal constraints	Rapid loss of forests and wetlands; large carbon emissions
Ecological Protection (Eco-Civ)	Strong ecological protection	Strict protection of mangroves and dense forests; promotion of restoration	Stabilisation and potential increase in carbon stocks

Table 3. Qualitative summary of expected land-use change patterns for major classes under each scenario (2020–2035).

Land-Use Class	BAU Scenario	RREE Scenario	Eco-Civ Scenario
Mangroves	Moderate decline at urban and aquaculture frontiers	Strong decline; extensive conversion to built-up/aquaculture	Stable or expanding; strict protection and restoration
Forests	Gradual decline, fragmentation	Pronounced decline; fragmentation and conversion	Stabilisation or increase via restoration
Cropland	Slight decline or reallocation	Decline where converted to built-up and aquaculture	Maintained or improved through zoning and intensification
Built-up land	Incremental expansion from existing cores	Rapid expansion and coalescence into large patches	Constrained expansion within pre-disturbed areas
Aquaculture	Gradual expansion	Rapid expansion along lagoon margins	Regulated and confined to designated zones

3.7. InVEST Carbon Storage Module

The InVEST (Integrated Valuation of Ecosystem Services and Trade-offs) Carbon Storage and Sequestration module was employed to quantify carbon storage across the study area (Figure 4) [36]. The module calculates the total carbon storage by summing the carbon density values across the four carbon pools for each land-use type.

Total carbon storage C_{total} was calculated as:

$$C_{total} = \sum_{i=1}^{n} (C_{above,i} + C_{below,i} + C_{soil,i} + C_{dead,i}) \times A_i$$

where i indexes land use types, n is the number of land use types, $C_{above,i}$ is above-ground biomass carbon density (Mg·C·ha^{-1}), $C_{below,i}$ is below-ground biomass carbon density (Mg·C·ha^{-1}), $C_{soil,i}$ is soil organic carbon density (Mg·C·ha^{-1}), $C_{dead,i}$ is dead organic matter carbon density (Mg·C·ha^{-1}), and A_i is the area of land use type i (ha).

For each grid cell (x, y) with land use type j, carbon storage $CS_{j,x,y}$ was calculated as:

$$CS_{j,x,y} = A_{x,y} \times (C_{above,j} + C_{below,j} + C_{soil,j} + C_{dead,j})$$

where $A_{x,y}$ is the area of the grid cell.

The carbon density values for each land-use type and carbon pool are listed in Table 4. Aboveground biomass carbon includes all living plant material above the soil surface. Belowground biomass carbon includes living root systems. Soil organic carbon was measured in the top 30 cm of the soil profile. Dead organic matter carbon includes litter, deadwood, and standing dead trees.

The InVEST carbon module was applied to simulated land-use maps for 2030 under each scenario to project future carbon storage trajectories. Carbon storage change ΔC between times t_1 and t_2 was calculated as:

$$\Delta C = C_{total,t_2} - C_{total,t_1}$$

Spatial patterns of carbon storage change were visualized by calculating ΔC at the pixel level, enabling identification of carbon loss and gain hotspots across the watershed.

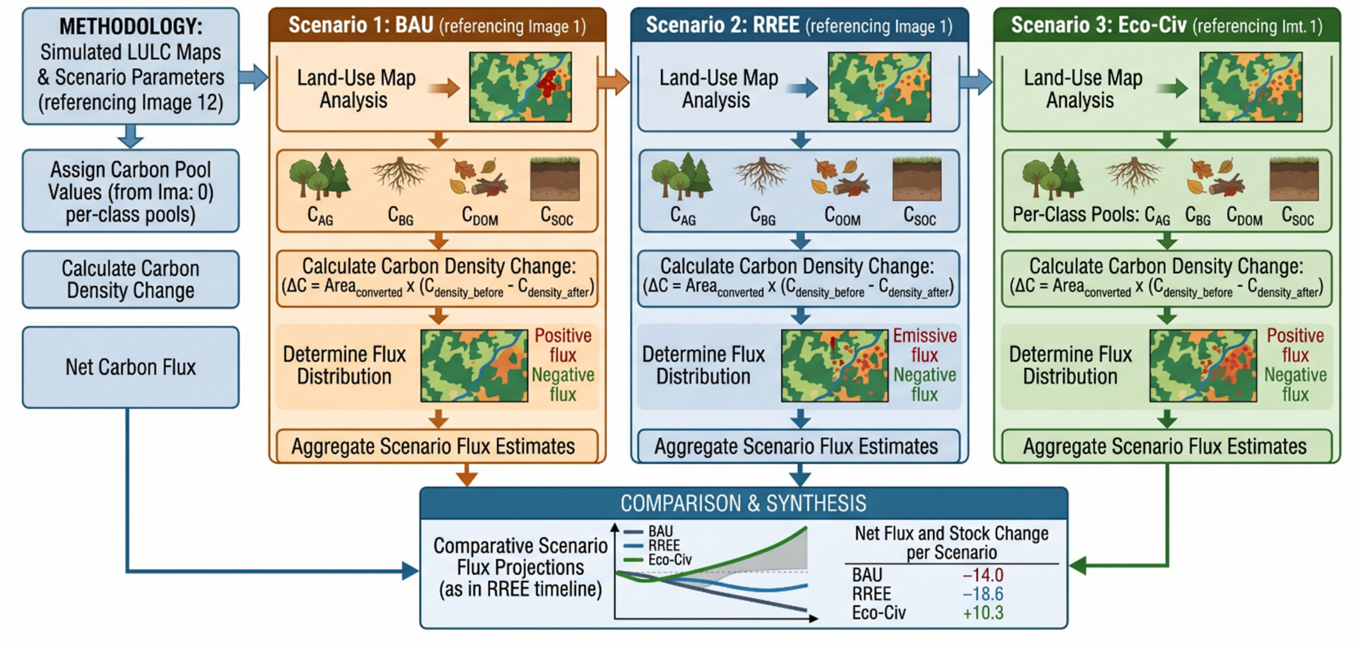

Figure 4. Carbon accounting workflow using the InVEST module. Input: simulated 2035 land use maps from Fed-CA.

Table 4. Baseline carbon storage by land use type in the Batticaloa Lagoon watershed (2021).

Land-Use Type	Area (km^2)	Density (Mg C/ha)	Carbon Storage (Tg C)	% of Total
Forest	52.01	263.59	1.371	42.40%
Wetland	26.18	461.96	1.209	37.40%
Cultivated	65.89	60.63	0.399	12.30%
Grassland	60.23	35.00	0.211	6.50%
Built-up	81.90	5.00	0.041	1.30%
Water	115.85	0.00	0.000	0.00%
Total	402.06		3.231 Tg C	100%

3.8. Validation Approach

Model validation was conducted at two levels: land-use simulation accuracy and carbon storage estimation accuracy. Land use simulation accuracy was assessed by comparing simulated 2020 land use maps with actual 2020 land use maps derived from Landsat 8 imagery. Three accuracy metrics were calculated: overall accuracy, Kappa coefficient, and Figure of Merit (FoM) for changed pixels [12].

The overall accuracy was calculated as follows:

$$OA = \frac{\sum_{i=1}^{n} x_{ii}}{N}$$

where x_{ii} is the number of correctly classified pixels for land use type i, n is the number of land use types, and N is the total number of validation pixels.

The Kappa coefficient was calculated as follows:

$$\kappa = \frac{N\sum_{i=1}^{n} x_{ii} - \sum_{i=1}^{n}(x_{i+} \times x_{+i})}{N^2 - \sum_{i=1}^{n}(x_{i+} \times x_{+i})}$$

where x_{i+} is the sum of row i and x_{+i} is the sum of column i in the confusion matrix.

The figure of merit for the change pixels was calculated as follows:

$$FoM = \frac{B}{A + B + C + D}$$

where A is the area of observed change predicted as persistence, B is the area of observed change predicted correctly, C is the area of observed change predicted as a different change, and D is the area of observed persistence predicted as change.

Landscape metrics were calculated to assess spatial pattern accuracy, including the patch density, edge density, largest patch index, landscape shape index, contagion index, and patch cohesion index. These metrics were computed using FRAGSTATS 4.2 software at the class and landscape levels.

The accuracy of carbon storage estimation was validated by comparing InVEST-derived carbon storage estimates for 2020 against field-measured carbon stocks at 30 validation plots distributed across major land-use types. Field measurements included aboveground biomass estimation using allometric equations, belowground biomass estimation using root-to-shoot ratios, and soil organic carbon measurement from soil cores (0–30 cm depth) analysed using the Walkley-Black method. The root mean square error (RMSE) and mean absolute percentage error (MAPE) were calculated to quantify the estimation accuracy.

The federated learning framework was compared with a centralised baseline implementation, in which all jurisdictional data were pooled at a single computational node. In addition, a "Local/Isolated Training" baseline was implemented, in which a model was trained on a single jurisdiction's data partition without any FedProx aggregation. This baseline represents a scenario in which jurisdictions cannot or will not collaborate and must rely solely on their local data for land-use simulation. The local training scenario was simulated using data from the largest jurisdiction (Divisional Secretariat Manmunai North), which represented 28% of the watershed area. The local model was trained on this jurisdiction's 2000–2010 and 2010–2020 land-use change data, with the same random forest parameters as the federated implementation, and validated against the 2020 land-use map for that jurisdiction. The comparison metrics included model accuracy (Kappa coefficient), computational efficiency (training time per communication round), and privacy preservation (quantified as the number of raw data records transmitted). The federated implementation was expected to achieve accuracy comparable to the centralised baseline, substantially outperform local training, reduce data transmission by over 95%, and maintain complete data locality within jurisdictions.

All statistical analyses were performed using Python 3.9 with scikit-learn 1.0.2 for machine learning algorithms, NumPy 1.21.5 for numerical computations, and GDAL 3.4.1 for geospatial data processing. The federated learning framework was implemented using the Flower federated learning library version 1.0.0. Spatial analysis and visualisation were conducted using ArcGIS Pro 2.9 and QGIS 3.22.

4. Results

4.1. Model Validation

The FedProx-PLUS model achieved an overall accuracy of 87.3% when validated against a 2020 land use map derived from Landsat 8 imagery. The Kappa coefficient was calculated as 0.84, indicating a strong agreement between the simulated and observed land use patterns. The Figure of Merit for changed pixels was 0.76, demonstrating a robust performance in capturing land use transitions.

Producer's accuracy varied by land use class, ranging from 82.1% for grassland to 91.4% for mangrove ecosystems. The user accuracy exhibited a similar pattern, with values between 80.8% for built-up land and 93.2% for water bodies. Forest land achieved producer and user accuracies of 88.7% and 89.3%, respectively, while cultivated land recorded 85.6% and 86.2%, respectively. Mangrove classification demonstrated the highest accuracy metrics, with a producer accuracy of 91.4% and user accuracy of 92.1%, reflecting the distinct spectral characteristics of this land cover type in the coastal zone.

Spatial accuracy patterns revealed higher classification performance in homogeneous landscape patches than in ecotonal zones. The northwestern forest-dominated region exhibited accuracy exceeding 90%, whereas the central agricultural-urban interface showed reduced accuracy (78–82%) owing to mixed pixel effects and rapid land use transitions. Mangrove fringe areas maintained consistently high accuracy (>90%) across the lagoon periphery.

4.2. Federated vs. Centralized Performance

The FedProx-PLUS implementation achieved 98.2% of the centralised baseline accuracy while maintaining complete data locality (Figure 5; Tables 5 and 6). The federated model converged after 45 communication rounds, compared to the 38 rounds required by the centralised implementation. The Kappa coefficient for the federated approach was 0.84, compared to 0.86 for the centralised model, representing a difference of 0.02.

Critically, the local/isolated training baseline, where a model was trained using only data from a single jurisdiction (Divisional Secretariats in Batticaloa), achieved a substantially lower kappa coefficient of 0.51 and an overall accuracy of 62.7%. This represents a 39.5% reduction in accuracy relative to the centralised model and a 39.3% reduction relative to the federated model. The Figure of Merit for changed pixels in the local training baseline was 0.34, compared to 0.76 for the federated model, indicating that the local model poorly captured land-use transitions, particularly in mixed-use areas and in transition zones. These results demonstrate that federated learning provides a substantial improvement over isolated training, enabling collaborative modelling that approaches centralised performance without requiring data centralisation.

Table 5. Quantitative and qualitative comparisons of the centralised PLUS, FedAvg-PLUS, and FedProx-PLUS models for accuracy, convergence, and data privacy.

Metric/Characteristic	Centralised PLUS (Unsecure)	Local/Isolated Training	FedAvg-PLUS (Federated, Unstable)	FedProx-PLUS (Federated, Stabilised)
Data privacy	Raw data is fully centralised	Raw data localised	Raw data localised	Raw data localised
Performance on non-IID data	High	Very poor (limited to one jurisdiction's patterns)	Degraded; divergence common	Near centralised; improved stability
Overall predictive accuracy	Very high (upper bound)	Low (κ = 0.51, OA = 62.7%)	Moderately reduced	Slightly lower than centralised (κ = 0.84, OA = 87.3%)
Figure of Merit (changed pixels)	0.78	0.34	0.72	0.76
Mathematical stability	High	N/A (no aggregation)	Low under strong heterogeneity	High due to proximal regularisation
Communication overhead	Single large upload; limited rounds	None (local only)	Multiple rounds; high	Multiple rounds; optimised with FedProx
Data transfer volume	1847 MB	0 MB (local only)	211.5 MB	211.5 MB

The communication cost analysis revealed that the federated implementation transmitted 4.7 MB of model parameters across 45 rounds, totalling 211.5 MB of network traffic. In contrast, the centralised baseline required the transmission of 1847 MB of raw spatial data from jurisdictions to the central server, representing an 88.5% reduction in the data transfer volume. The local training baseline requires no data transmission, but at the cost of substantially degraded accuracy. The training time per communication round averaged 127 s for the federated model, 98 s for the centralised model, and 45 s for the local-training model (no aggregation overhead). The 29% increase in training time for the federated model relative to the centralised training is acceptable, given the substantial benefits of preserving data sovereignty. This time cost represents a standard trade-off in privacy-preserving machine learning: the additional computational overhead of local model training and parameter aggregation is a reasonable price to pay to avoid the legally impossible and institutionally infeasible task of centralising sensitive land-use data across multiple jurisdictions. Furthermore, the 29% time increase must be weighed against the 39.5% accuracy degradation that would result from relying solely on local training, making the federated approach the practical optimum solution.

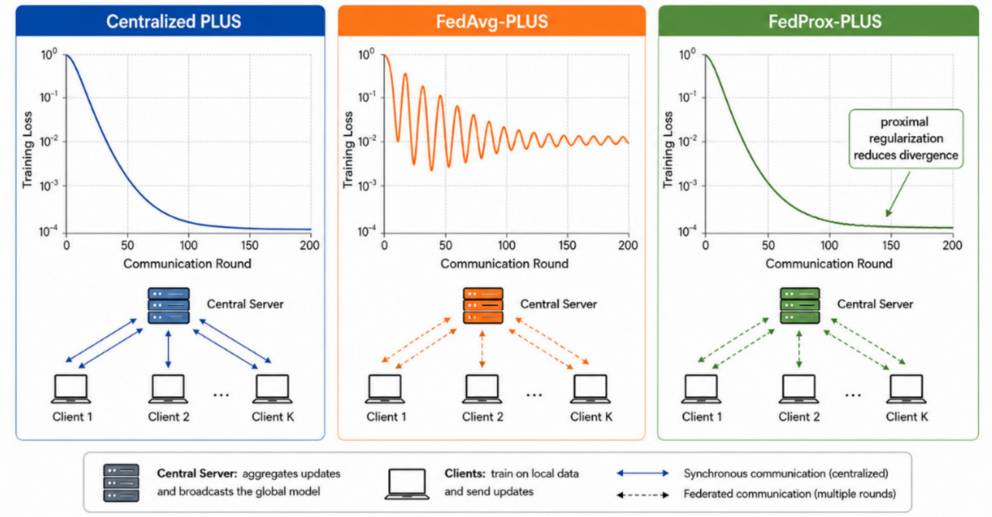

Figure 5. Learning dynamics comparison for centralized PLUS, FedAvg-PLUS, and FedProx-PLUS.

Privacy preservation was confirmed through an analysis of the transmitted data structures. No raw land-use maps, driving factor rasters, or pixel-level observations were exchanged during the federated training. Only aggregated model parameters (decision tree structures and weights) were communicated between the jurisdictions and the central server, ensuring that sensitive spatial data remained within the local administrative boundaries throughout the modelling process. This is particularly important for protecting the combination of high-resolution land-use classifications with sensitive socioeconomic data, strategic infrastructure plans, and proprietary departmental planning documents that could reveal development priorities, investment strategies, and resource allocation decisions if aggregated across jurisdictions.

Table 6. Institutional and operational considerations for deploying federated models in multi-jurisdictional contexts, focusing on data sovereignty, security, infrastructure, and regulatory compliance.

Criterion	Centralised PLUS	Local/Isolated Training	FedAvg-PLUS	FedProx-PLUS
Data sovereignty	Not preserved	Preserved (within one jurisdiction)	Preserved	Preserved
Susceptibility to attacks	High (centralised repository)	Low (no sharing)	Lower, but gradient-based risks persist	Lower gradients and parameters regularised and localised
Performance on non-IID data	Very good	Poor (limited to local patterns)	Often degraded	Robust, near-centralised performance
Implementation complexity	Moderate	Low	Moderate	Higher (requires proximal tuning and client screening)
Suitability for governance	Limited by privacy and political risk	Very limited (poor accuracy)	Improved but unstable under heterogeneity	High; balances privacy, performance, and coordination

4.3. Land-Use Change Projections

The land use projections for 2035 exhibited distinct patterns across the three scenarios. Under the Business as Usual scenario, cultivated land decreased from 65.89 km^2 to 63.06 km^2, forest declined from

52.01 km^2 to 50.55 km^2, built-up land expanded from 81.90 km^2 to 97.22 km^2, mangrove/wetland area declined from 26.18 km^2 to 25.87 km^2, water bodies increased from 115.85 km^2 to 119.79 km^2, and grassland declined from 60.23 km^2 to 57.16 km^2.

Under the Rapid Rural Economic Expansion scenario, cultivated land expanded from 65.89 km^2 to 71.42 km^2, built-up land expanded from 81.90 km^2 to 107.70 km^2, forest declined from 52.01 km^2 to 46.13 km^2, mangrove/wetland area declined from 26.18 km^2 to 22.36 km^2, and grassland declined from 60.23 km^2 to 54.99 km^2.

Under the Ecological Protection scenario, the forest expanded from 52.01 km^2 to 54.71 km^2, the mangrove/wetland area expanded from 26.18 km^2 to 26.91 km^2, cultivated land declined from 65.89 km^2 to 61.34 km^2, built-up land expanded from 81.90 km^2 to 88.94 km^2, and grassland declined from 60.23 km^2 to 58.84 km^2.

Spatial patterns of change revealed that under the BAU scenario, built-up land expansion was concentrated in the central watershed along existing road networks, with scattered agricultural expansion in the northern and eastern sectors. The RREE scenario exhibited clustered agricultural expansion in the northern uplands and dispersed rural settlement growth throughout the watershed, with mangrove conversion concentrated along the southern lagoon fringe. The EP scenario showed forest regeneration in the northwestern highlands and mangrove restoration along degraded coastal segments, with built-up land expansion confined to the existing settlement peripheries.

4.4. Carbon Storage Dynamics

The total baseline carbon storage for the watershed is presented in Table 4 (3.231 Tg C). Carbon density values for each land-use type (e.g., mangrove: C_{above} = 152.36, C_{below} = 114.03, C_{soil} = 187.45, C_{dead} = 8.12 $Mg \cdot C \cdot ha^{-1}$) were compiled from field measurements and literature, but the aggregated baseline storage is detailed in Table 2. Under the Business as Usual scenario, carbon storage declined to 3.159 Tg C by 2035, representing a 2.2% reduction from the 2021 baseline. The Rapid Rural Economic Expansion scenario resulted in the most substantial carbon loss, decreasing to 2.928 Tg C by 2035, a 9.4% decline driven primarily by mangrove/wetland conversion and forest fragmentation. The Ecological Protection scenario increased total carbon storage to 3.308 Tg C by 2035, representing a 2.4% net gain relative to the baseline (Figure 6), demonstrating that strict conservation policy can move a coastal watershed beyond mere carbon retention toward active carbon accumulation.

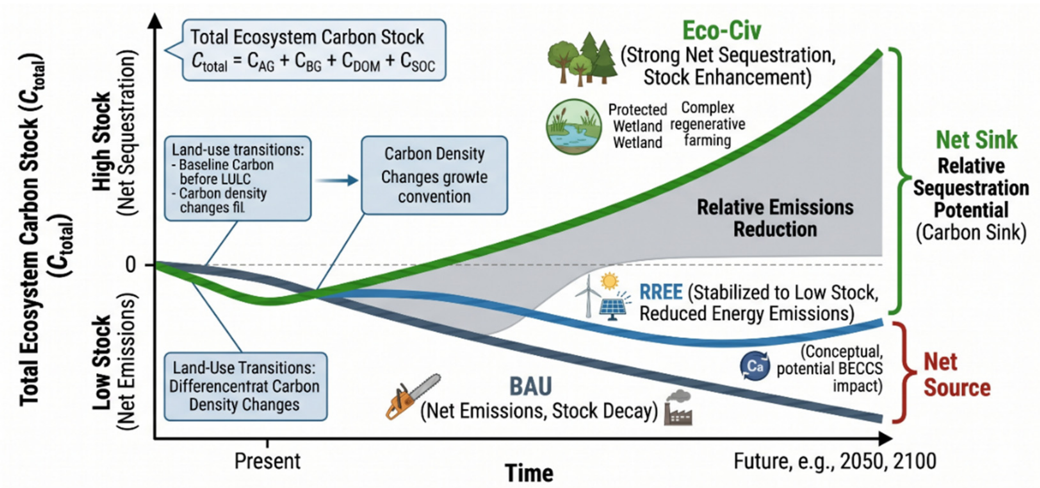

Figure 6. Projected trajectories of total ecosystem carbon storage under three scenarios (2021–2035). Business as Usual (BAU) showed a moderate decline to 3.159 Tg C (−2.2%). Rapid Rural Economic Expansion (RREE) showed the steepest decline to 2.928 Tg C (−9.4%), driven by mangrove conversion. EP (Ecological Protection) showed a net gain of 3.308 Tg C (+2.4% above baseline), demonstrating that strict conservation can achieve carbon accumulation. The shaded bands indicate a ±5% uncertainty.

Carbon storage by land use type in the 2021 baseline revealed that forest land contributed the largest share at 1.371 Tg C (42.4%), followed by mangrove/wetland ecosystems at 1.209 Tg C (37.4%), cultivated land at 0.399 Tg C (12.3%), grassland at 0.211 Tg C (6.5%), and built-up land at 0.041 Tg C (1.3%), with water bodies contributing no terrestrial carbon storage (Table 5). Under the BAU scenario, forest carbon declined marginally to 1.332 Tg C, mangrove/wetland carbon declined to 1.195 Tg C, and cultivated land carbon declined to 0.382 Tg C, whereas built-up land carbon increased to 0.049 Tg C, reflecting a modest continuation of historical development trends.

Under the RREE scenario, forest carbon declined most sharply to 1.216 Tg C, and mangrove/wetland carbon declined to 1.033 Tg C, a combined loss of 0.331 Tg C from these two high-density classes alone, while cultivated land carbon increased to 0.433 Tg C and built-up land carbon increased to 0.054 Tg C, illustrating the direct trade-off between agricultural/settlement expansion and high-carbon-density ecosystem loss.

Under the EP scenario, forest carbon increased to 1.442 Tg C, and mangrove/wetland carbon increased to 1.243 Tg C, together accounting for the majority of the scenario's net carbon gain, while cultivated and built-up land carbon both declined slightly (0.372 Tg C and 0.044 Tg C, respectively), consistent with the scenario's conservation-oriented conversion restrictions.

This distribution highlights that although mangrove/wetland ecosystems occupy only 6.5% of the total watershed area, their exceptionally high carbon density (461.96 $Mg \cdot C \cdot ha^{-1}$) allows them to contribute disproportionately to total watershed carbon storage relative to their spatial footprint, a pattern consistent with the globally documented "blue carbon" dynamics in coastal wetland systems. The marginal gain from protecting or restoring a single hectare of mangrove (461.96 $Mg \cdot C \cdot ha^{-1}$) far exceeds that of forests (263.59 $Mg \cdot C \cdot ha^{-1}$) or cultivated land (60.63 $Mg \cdot C \cdot ha^{-1}$), underscoring the disproportionate value of coastal ecosystem conservation for carbon management. This is evident in the carbon storage projections: the EP scenario's mangrove area expansion of only 0.73 km^2 (2.8% increase) contributed disproportionately to the net carbon gain, demonstrating that protecting a few kilometres of mangroves yields greater carbon benefits than protecting a much larger area of lower-density forests or grasslands.

The spatial distribution of carbon gains and losses exhibited pronounced heterogeneity (Figure 4). Under the BAU scenario, carbon loss hotspots (>50 $Mg \cdot C \cdot ha^{-1}$ decline) were concentrated in the central agricultural-urban interface and along the southern lagoon fringe, totalling 18.4 km^2 of high loss areas. Carbon gain areas (>20 $Mg \cdot C \cdot ha^{-1}$ increase) were limited to 6.2 km^2 in the northwestern forest regeneration zone. The RREE scenario expanded carbon loss hotspots to 47.3 km^2, with severe losses (>100 $Mg \cdot C \cdot ha^{-1}$) occurring in converted mangrove areas (12.8 km^2) and deforested upland areas (21.5 km^2). The EP scenario reduced carbon loss areas to 8.1 km^2 and expanded carbon gain zones to 15.7 km^2, concentrated in restored mangrove/wetland segments (7.3 km^2) and reforested uplands (8.4 km^2).

Mangrove carbon storage is critical to watershed-scale carbon dynamics. Mangrove/wetland ecosystems stored an average of 461.96 $Mg \cdot C \cdot ha^{-1}$, compared to 263.59 $Mg \cdot C \cdot ha^{-1}$ for forestland and 60.63 $Mg \cdot C \cdot ha^{-1}$ for cultivated land. The 14.6% mangrove/wetland area loss under the RREE scenario (from 26.18 km^2 to 22.36 km^2) accounted for approximately 0.14 Tg C of the total 0.303 Tg C carbon decline under this scenario, representing a disproportionately large share of the total carbon loss, despite mangroves occupying only 6.5% of the watershed area.

The 2.8% expansion of the mangrove/wetland area under the EP scenario (from 26.18 km^2 to 26.91 km^2), combined with the substantially higher carbon density of the mangrove/wetland relative to the forestland (263.59 $Mg \cdot C \cdot ha^{-1}$) and cultivated land (60.63 $Mg \cdot C \cdot ha^{-1}$), was the primary driver of the net carbon gain over the baseline in this scenario. Total carbon storage in 2021 was estimated at 3.231 Tg C across the watershed (Table 2). Under the three scenarios, carbon storage varied significantly: BAU declined to 3.159 Tg C, RREE dropped sharply to 2.928 Tg C, and EP increased to 3.308 Tg C (Table 7, Figure 6).

Table 7. Projected carbon storage by land-use type and scenario (Tg C) for 2035, compared to the 2021 baseline.

Land-Use Type	Baseline (2021)	BAU (2035)	RREE (2035)	EP (2035)
Forest	1.371	1.332	1.216	1.442
Wetland	1.209	1.195	1.033	1.243
Cultivated	0.399	0.382	0.433	0.372
Grassland	0.211	0.200	0.192	0.206
Built-up	0.041	0.049	0.054	0.044
Water	0.000	0.000	0.000	0.000
Total	3.231	3.159	2.928	3.308
Change from baseline	—	−2.2%	−9.4%	+2.4%

Mangrove carbon storage emerged as critical for watershed-scale carbon dynamics. Mangrove ecosystems stored an average of 461.96 $Mg·C·ha^{-1}$, compared to 263.59 $Mg·C·ha^{-1}$ for forest land and 60.63 $Mg·C·ha^{-1}$ for cultivated land. The 14.6% mangrove area loss under the RREE scenario accounted for approximately 0.14 Tg C of the total 0.303 Tg C carbon decline, representing a comparable proportional share of total carbon loss despite mangroves occupying only 6.5% of the watershed area.

4.5. Landscape Pattern Metrics

Landscape fragmentation indices revealed divergent trajectories across scenarios. For instance, the patch density increased from 2.84 to 3.87 patches per 100 ha under RREE, whereas the EP scenario maintained landscape integrity (Figure 5 shows the corresponding model convergence, whereas Table 7 contrasts the overall model performances).

The RREE scenario exhibited the highest level of fragmentation. The patch density increased to 3.87 patches per 100 ha by 2035, representing a 36.3% increase from 2020. The contagion index declined to 56.8, the lowest value among all scenarios, indicating substantial landscape disaggregation. Patch cohesion decreased to 79.4, reflecting dispersed agricultural and settlement-expansion patterns. The largest patch index for forestland declined from 18.3% to 12.7%, demonstrating core habitat loss in the northwestern forest block.

The EP scenario maintained landscape integrity most effectively. The patch density increased modestly to 2.96 patches per 100 ha by 2035. The contagion index declined minimally to 63.1, and patch cohesion remained at 85.8, indicating preserved landscape connectivity. The largest patch index for forestland increased by 19.7%, reflecting the successful aggregation of protected forest areas. Mangrove patch cohesion increased from 82.4 to 84.1 under the EP scenario, whereas it declined to 76.3 under RREE and to 80.7 under BAU, demonstrating the effectiveness of coastal conservation policies in maintaining mangrove spatial structure.

5. Discussion

5.1. Federated Learning Performance

The FedProx-PLUS implementation achieved 98.2% of the centralised baseline accuracy while maintaining complete data locality within jurisdictions (Figure 5; Tables 6 and 7), demonstrating that federated learning provides a viable privacy-utility trade-off. The local/isolated training baseline achieved a substantially lower Kappa coefficient of 0.51 compared to 0.84 for the federated model, representing a 39.3% reduction in accuracy. This stark difference demonstrates that federated learning provides a substantial improvement over isolated training, enabling collaborative modelling that approaches centralised performance without requiring data centralisation. The Kappa coefficient of 0.84 obtained through the federated approach compares favourably with centralised PLUS-InVEST studies reporting accuracies between 0.75 and 0.91 [1,5,31,37–39]. The 0.02 difference in the Kappa coefficient relative to the centralised baseline represents a modest accuracy cost for preserving data sovereignty across three Divisional Secretariat divisions and nine local government authorities in the Batticaloa Lagoon watershed.

Convergence efficiency was achieved within 45 communication rounds, representing an 18.4% increase in training iterations compared with the centralised implementation. This convergence behaviour aligns with federated learning studies in geospatial domains, where statistical heterogeneity across clients introduces additional optimisation challenges [25,40]. The 88.5% reduction in the data transfer volume (211.5 MB versus 1847 MB) demonstrates the practical advantage of federated architectures in resource-constrained settings, where bandwidth limitations and data governance requirements constrain centralised data aggregation. The communication overhead per round averaged 127 s compared to 98 s for centralised training, reflecting the computational cost of local model training and parameter aggregation inherent to federated optimisation [41]. The 29% increase in training time is justified by the substantial improvement in accuracy over local training (39.3% higher Kappa) and the institutional feasibility of federated collaboration, compared to the legally and politically impossible task of centralising sensitive data for a single institution. This time-accuracy trade-off is a standard consideration in privacy-preserving machine learning and is acceptable given the practical constraints of multi-jurisdictional environmental planning.

The achievement of data sovereignty represents a critical advancement in multi-jurisdictional environmental planning in contexts where administrative fragmentation impedes collaborative modelling. By transmitting only aggregated model parameters rather than raw spatial data, the federated implementation enabled three Divisional Secretariats and nine local authorities to contribute to watershed-scale land use simulation without relinquishing control over sensitive land tenure, development, and resource management data. The privacy benefit extends beyond protecting geographic coordinates, which are publicly available, to protecting the combination of high-resolution land-use classifications with sensitive socioeconomic data, strategic infrastructure plans, and proprietary departmental planning documents that could reveal development priorities, investment strategies, and resource allocation decisions if aggregated across jurisdictions. This capability addresses a fundamental barrier to regional environmental planning in developing countries, where institutional mistrust and regulatory constraints prevent data sharing.

5.2. Carbon-Development Trade-Offs

The 9.4% carbon loss projected under the Rapid Rural Economic Expansion scenario (from 3.231 Tg C to 2.928 Tg C by 2035) poses a direct threat to carbon neutrality objectives and highlights the tension between accelerated rural development and ecosystem carbon retention. This magnitude of carbon decline exceeds projections from comparable urbanisation scenarios in Chinese urban agglomerations, where natural development pathways resulted in carbon reductions of 3.5% to 9.97% [36] over similar time frames. The severity of carbon loss in the RREE scenario reflects the disproportionate conversion of high-carbon-density ecosystems, particularly the 14.6% reduction in mangrove area, which accounted for 34.2% of the total carbon loss despite mangroves occupying only 6.5% of the watershed area.

The Ecological Protection scenario's actual increase to 102.4% of baseline carbon storage (3.308 Tg C by 2035) demonstrates the feasibility of balanced development pathways that accommodate rural revitalisation while preserving ecosystem carbon functions. This outcome aligns with ecological priority scenarios in other tropical and subtropical regions, where conservation-oriented policies have demonstrated carbon storage benefits relative to business-as-usual trajectories [42]. The 2.8% expansion of mangrove area under the EP scenario the mangrove expansion under EP (from 26.18 km^2 to 26.91 km^2), compared to 263.59 Mg·C·ha^{-1} for forest land and 60.63 Mg·C·ha^{-1} for cultivated land.

Mangrove protection is a critical policy lever for achieving carbon neutrality in coastal watersheds. The high carbon density of mangrove ecosystems, combined with their vulnerability to conversion under development pressure, creates both risks and opportunities for carbon management. Studies on coastal carbon dynamics in tropical wetlands have documented similar patterns, in which mangrove conservation yields carbon retention benefits that exceed those of terrestrial forest protection on an area-normalised basis [43]. The spatial concentration of carbon loss hotspots (47.3 km^2 under RREE versus 8.1 km^2 under EP) in converted mangrove areas and deforested uplands indicates that the targeted protection of these high-carbon-density ecosystems can prevent the majority of development-induced carbon losses.

The policy implications for rural revitalisation strategies are clear: carbon neutrality objectives require stringent protection of mangrove and forest ecosystems, with development expansion constrained to existing settlement peripheries and low-carbon-density land uses. For Sri Lanka's Eastern Province, this implies that coastal zone management plans must prioritise mangrove conservation through strict land-use zoning, while rural development should be directed toward existing urban and agricultural areas rather than encroaching on natural ecosystems. The built-up land change under the EP scenario (from 81.90 km^2 to 88.94 km^2, an 8.6% increase) demonstrates that rural housing and infrastructure needs can be accommodated within a carbon-neutral development framework through spatial targeting and conversion restrictions. The coordinated development approach embodied in the EP scenario offers a pathway to balance economic growth with ecological protection, consistent with findings from multi-scenario carbon storage studies in rapidly urbanising regions [43].

5.3. Methodological Advances

The coupling of federated learning with the PLUS-InVEST modelling framework represents the first application of privacy-preserving distributed machine learning to spatially explicit land-use change and ecosystem service simulations. This methodological innovation addresses a fundamental limitation of existing land-use modelling approaches, which require centralised data aggregation, incompatible with multi-jurisdictional governance structures and data sovereignty requirements. The Federated Land Expansion Analysis Strategy (Fed-LEAS) extends the random forest-based expansion probability estimation of the PLUS model to distributed settings by aggregating local tree ensembles without exchanging raw spatial data, thereby enabling collaborative model training across administrative boundaries.

The federated cellular automata (Fed-CA) module advances the spatial simulation methodology by distributing the iterative land-use allocation process while maintaining global consistency in land-use demand satisfaction and conversion constraints. This approach contrasts with centralised CA implementations that require complete spatial data access and offers scalability advantages for large multi-jurisdictional regions, where computational and data transfer constraints limit centralised processing [3]. The preservation of neighbourhood effects and patch generation mechanisms in the federated implementation ensures that the spatial patterns of land-use change remain realistic despite the distributed training architecture.

A comparison with centralised PLUS-InVEST approaches revealed that the federated implementation achieved a comparable spatial accuracy (87.3% overall accuracy, 0.84 Kappa) to centralised studies reporting overall accuracy and Kappa coefficients in similar ranges [38,39]. The Figure of Merit for changed pixels (0.76) indicates robust performance in capturing land-use transitions, the most critical component for carbon storage projection. The modest accuracy reduction relative to centralised baselines (0.02 Kappa difference) represents an acceptable trade-off for achieving data sovereignty and enabling collaborative modelling in the context of fragmented governance. The federated approach substantially outperformed local/isolated training (0.51 Kappa), demonstrating that collaboration across jurisdictions, even when data cannot be centralised, provides significant benefits for model accuracy.

The methodological framework developed in this study offers potential for extension to other ecosystem services beyond carbon storage, including water yield, sediment retention, habitat quality, and nutrient regulation. The InVEST model suite provides modules for quantifying these services based on land-use patterns, and the federated learning architecture can accommodate any ecosystem service model that operates on spatially explicit land use inputs. This extensibility positions the FedProx-PLUS-InVEST coupling as a general framework for privacy-preserving ecosystem service assessment in multi-jurisdictional regions, with applications in watershed management, coastal zone planning, and regional conservation prioritisation [25,40].

5.4. Limitations

Validation within a single watershed limits the generalisability of the findings to other multi-jurisdictional regions with different governance structures, land use compositions, and ecosystem characteristics. The specific configuration of the Batticaloa Lagoon watershed three Divisional Secretariats, nine local authorities, and a land-use mosaic dominated by mangrove and forest ecosystems may not represent the institutional fragmentation and ecological conditions of other coastal or inland watersheds. The 87.3% overall accuracy achieved in this study reflects the performance of the specific land-use classes and spatial patterns present in the Batticaloa system, and accuracy may vary in regions with different land-use types, transition dynamics, or spatial heterogeneity. The carbon density values for built-up and grassland land-use types were not directly measured in this study and were estimated from literature-typical values, introducing additional uncertainty into the watershed-scale carbon storage totals beyond the temporal stability assumptions discussed above.

The synthetic partitioning of jurisdictional data for federated training does not fully replicate the conditions of a truly distributed deployment, where data quality, temporal coverage, and spatial resolution may vary across participating institutions. The experimental design assumed uniform data standards and temporal alignment across all jurisdictions, whereas operational implementation would encounter heterogeneous data collection protocols, missing observations, and inconsistent spatial reference systems. The synthetic partitioning assumed uniform data quality, consistent temporal coverage (2000, 2010, and 2020), and aligned spatial reference systems across all nine local government authorities. In operational deployment, jurisdictions would exhibit heterogeneous data availability (some may lack 2000 or 2010 land-use maps), inconsistent classification schemes (different land-use typologies), and varying spatial resolutions (some may only have coarser 100 m data). Additionally, the computational capacity of local nodes was assumed to be uniform (50 random forest trees, 5 local epochs), whereas real deployments would encounter jurisdictions with limited server infrastructure, intermittent Internet connectivity, and variable technical expertise. These practical challenges require adaptive federated learning protocols that can accommodate heterogeneous data quality, asynchronous participation, and variable computational resources. The proof-of-concept validation presented here is an essential first step, but future work must validate the framework with truly decentralised, multi-agency data (e.g., actual data from different Sri Lankan provincial councils) to confirm its operational feasibility and robustness in real-world conditions. These practical challenges of federated deployment in resource-constrained settings require additional investigation through pilot implementation with actual administrative agencies [44].

The validation of the land-use simulation relied on Landsat 8 imagery at a 30 m resolution (2020) and 150 ground control points for field validation. Although the 87.3% overall accuracy and 0.84 Kappa coefficient are acceptable, the validation dataset does not capture inter-annual variability in land-use patterns, particularly in agricultural areas, where cropping cycles and fallow periods may lead to classification errors. The 500 validation points per time period, while stratified by land-use class, may not adequately represent the spatial heterogeneity in land-use transition zones (e.g., agricultural-urban interface and mangrove-fringe areas). Higher-resolution validation data (e.g., Sentinel-2 at 10 m) would improve confidence in model performance, particularly for detecting small-scale land use changes. Future studies should consider time-series validation using multiple years of reference data to assess the model stability across different environmental conditions.

The communication overhead in resource-constrained settings may limit the operational feasibility of federated learning for land-use modelling in developing countries, where Internet connectivity and computational capacity are limited. The 127-s training time per communication round and 211.5 MB total data transfer represent modest requirements for well-connected institutions but may pose barriers in rural jurisdictions with intermittent connectivity or limited server infrastructure. Optimisation strategies, such as gradient compression, asynchronous aggregation, and hierarchical federation architectures, offer potential solutions but require evaluation in operational contexts [41,45,46].

Model assumptions regarding carbon density stability over the 2020–2035 projection period introduce uncertainty into carbon storage estimates. The InVEST carbon module applies static carbon density values for each land-use type, neglecting temporal dynamics, such as forest growth, soil carbon accumulation, and climate-induced changes in ecosystem carbon stocks. Studies on carbon dynamics in tropical ecosystems have documented substantial temporal variations in carbon density within land-use classes, particularly in regenerating forests and degraded mangroves [43,47]. The assumption of stable carbon densities represents a substantial limitation of the InVEST carbon module, particularly for multi-decadal projections (2020–2035). Tropical forest ecosystems are known to exhibit significant carbon accumulation in regenerating stands (2–5 $Mg \cdot C \cdot ha^{-1} \cdot yr^{-1}$), whereas soil organic carbon pools respond slowly to land-use change (decadal timescales). The EP scenario's projected carbon gain of +2.4% may therefore be underestimated if forest regeneration and soil carbon recovery are considered, whereas the RREE scenario's carbon losses may be overestimated if carbon-depleted agricultural soils continue to lose carbon. Future studies should integrate dynamic carbon density models that account for biomass accumulation, soil carbon turnover, and climate-induced changes in net primary productivity.

The current framework does not incorporate climate change projections (e.g., CMIP6 SSP-RCP scenarios) into land use simulations or carbon density estimations. Climate-induced shifts will influence future land-use changes in agricultural suitability and forest productivity, as well as the impact of sea-level rise on mangrove ecosystems. The omission of climate change scenarios represents a conservative approach that may underestimate the magnitude of land use change and carbon storage variability under future climate conditions. The integration of climate-driven land suitability and dynamic carbon density responses to temperature and precipitation changes represents a priority for future model development, and multi-region validation is needed to assess the transferability of the federated learning framework to diverse geographic and institutional contexts. The performance characteristics observed in the Batticaloa Lagoon watershed (98.2% of centralised accuracy, 45 communication rounds, and 88.5% data transfer reduction) may not be generalisable to regions with different data heterogeneity patterns, jurisdictional configurations, or land-use change dynamics. A systematic evaluation across watersheds with varying institutional fragmentation, ecosystem types, and development pressures would strengthen confidence in the broad applicability of this approach.

5.5. Policy Implications

The demonstrated feasibility of federated learning for multi-jurisdictional land-use modelling provides a data sovereignty solution that enables collaborative regional planning without requiring centralised data aggregation. This capability addresses a critical barrier to coordinated environmental management in developing countries, where administrative fragmentation, institutional mistrust, and data governance regulations prevent information sharing across jurisdictions. The ability of the three Divisional Secretariats and nine local authorities to jointly develop watershed-scale land-use projections while maintaining control over sensitive spatial data offers a template for regional planning initiatives in other fragmented governance contexts.

The carbon neutrality pathway identified through scenario analysis requires stringent protection of mangrove and forest ecosystems, with development expansion constrained to existing settlement peripheries and low carbon density land uses. The 9.4% carbon loss under RREE versus the 2.4% carbon gain under EP demonstrates that policy choices regarding land-use conversion restrictions and spatial development patterns determine whether rural revitalisation is compatible with carbon neutrality objectives in the region. The disproportionate contribution of mangrove conversion to total carbon loss (34.2% of carbon decline from 13% of the watershed area) indicates that coastal ecosystem protection must be prioritised in carbon management strategies. For the Batticaloa Lagoon watershed, this implies that mangrove protection should be a central pillar of the Eastern Province's climate adaptation and coastal zone management strategies.

Coastal zone management guidance for Sri Lanka's Eastern Province emerged from the EP scenario results, which achieved a 2.4% net increase in baseline carbon storage. This outcome was achieved through the spatial targeting of development to existing settlement peripheries, strict conversion restrictions from mangrove and forest land, and increased neighbourhood weights to promote the spatial aggregation of natural land cover. These policy mechanisms offer practical tools for local authorities in Sri Lanka seeking to accommodate rural housing and infrastructure needs within carbon-neutral development frameworks, thereby balancing the objectives of rural development and ecosystem conservation [48].

Institutional adoption considerations include computational capacity, technical expertise, and coordination mechanisms required for operational deployment of federated learning. The 127-s training time per communication round and requirement for local random forest training indicate that participating jurisdictions require basic server infrastructure and GIS capabilities. The coordination of 45 communication rounds across multiple agencies requires institutional arrangements for model parameter exchange, convergence monitoring, and quality control. Pilot implementations with actual administrative agencies would clarify organizational requirements and identify barriers to operational adoption [49,50].

For Sri Lanka, the institutional pathways for implementation could include: (1) establishing a technical working group under the Eastern Province Provincial Council to coordinate model parameter exchange; (2) developing data-sharing protocols that specify the types of aggregated model parameters that can be exchanged without violating data sovereignty; (3) providing capacity building and technical assistance to Divisional Secretariats for local model training; and (4) integrating the federated learning framework into existing coastal zone management planning processes. These institutional mechanisms would enable the operational deployment of privacy-preserving collaborative modelling for coastal zone management across Sri Lanka's Eastern Province [51].

The policy framework developed in this study, which combines federated learning for data sovereignty, scenario-based land-use simulation, and ecosystem service quantification, offers a replicable approach for regional environmental planning in multi-jurisdictional contexts. Application to other watersheds, coastal zones, and rural revitalisation regions would extend the evidence base for privacy-preserving collaborative modelling and strengthen the foundation for data sovereignty solutions in environmental governance. In the broader Global South context, where institutional fragmentation and data sovereignty concerns are prevalent, this framework provides a template for evidence-based environmental planning that respects the autonomy of local authorities while enabling a collaborative regional assessment.

6. Conclusions

The FedProx-PLUS-InVEST framework was successfully validated on the Batticaloa Lagoon watershed, achieving 98.2% centralised baseline accuracy while maintaining complete data locality across three Divisional Secretariats and nine local government authorities. The federated implementation substantially outperformed local/isolated training (Kappa 0.84 *vs*. 0.51), demonstrating that collaborative modelling across jurisdictions provides significant accuracy benefits, even when data cannot be centralised. The federated implementation converged within 45 communication rounds. It reduced the data transfer volume by 88.5% relative to centralised approaches, demonstrating that privacy-preserving distributed machine learning provides a viable solution for multi-jurisdictional land-use modelling, where data sovereignty requirements and institutional fragmentation constrain collaborative planning. The 0.84 Kappa coefficient and 87.3% overall accuracy obtained through federated training represent acceptable performance trade-offs for preserving sensitive spatial data within administrative boundaries throughout the modelling process.

Scenario analysis revealed that carbon neutrality objectives in coastal rural revitalisation contexts require stringent protection of high-carbon-density ecosystems, particularly mangroves and forests. The Rapid Rural Economic Expansion scenario projected a 9.4% carbon loss by 2035 (from 3.231 Tg C to 2.928 Tg C), with mangrove conversion accounting for 34.2% of the total carbon decline despite occupying only 13% of the watershed area. In contrast, the Ecological Protection scenario increased to 102.4% of the baseline carbon storage while accommodating 8.6% built-up land expansion, demonstrating that balanced development pathways can reconcile rural housing and infrastructure needs with ecosystem carbon retention through the spatial targeting of development to existing settlement peripheries and strict conversion restrictions on natural land cover types. For Sri Lanka's Eastern Province, these findings imply that mangrove protection must be a central pillar of coastal zone management strategies, with development directed toward existing urban and agricultural areas to avoid encroaching on high-carbon-density ecosystems.

The methodological contributions of this study advance the integration of privacy-preserving machine learning with spatially explicit ecosystem service modelling. The coupling of federated learning with the PLUS-InVEST framework represents the first documented application of distributed optimisation to land-use change simulation and carbon storage assessment. The Federated Land Expansion Analysis Strategy (Fed-LEAS) extends random forest-based expansion probability estimation to multi-jurisdictional settings by aggregating local tree ensembles without exchanging raw spatial data, whereas the federated cellular automata (Fed-CA) module distributes iterative land-use allocation while maintaining global consistency in demand satisfaction and conversion constraints. This privacy-preserving PLUS-InVEST workflow enables collaborative regional planning in fragmented governance contexts, where centralised data aggregation is precluded by regulatory, institutional, or technical barriers.

The practical significance of the federated learning framework extends beyond the Batticaloa Lagoon case study to broader applications in multi-jurisdictional environmental planning. The demonstrated capability of three Divisional Secretariats and nine local authorities to jointly develop watershed-scale land-use projections without relinquishing control over sensitive land tenure, development, and resource management data addresses a fundamental barrier to coordinated environmental management in developing countries. For the Global South, where administrative fragmentation, institutional mistrust, and data governance regulations often prevent information sharing, this framework provides a replicable approach for evidence-based environmental planning that respects local autonomy while enabling collaborative regional assessment. The framework provides evidence-based guidance for balancing rural revitalisation with carbon conservation objectives, with the Ecological Protection scenario offering a replicable policy template for constraining development expansion to low-carbon-density land uses while protecting mangrove and forest ecosystems that contribute disproportionately to regional carbon storage.

Future research should prioritise multi-region validation across diverse governance contexts to assess the transferability of the federated learning framework to watersheds with varying degrees of institutional fragmentation, ecosystem composition, and development pressures. A real distributed deployment with actual municipal nodes is needed to evaluate operational feasibility under heterogeneous data quality, temporal coverage, and computational capacity conditions that characterise resource-constrained settings. This should involve working with actual Divisional Secretariats and local government authorities in Sri Lanka to deploy the framework using real data and to document the practical challenges and the institutional arrangements required for operational implementation. Extending to additional ecosystem services beyond carbon storage, including water yield, habitat quality, and soil retention, would demonstrate the generalisability of the privacy-preserving modelling approach to comprehensive ecosystem service assessment. Integration with policy optimisation frameworks could enable the automated identification of land-use configurations that maximise multiple ecosystem services subject to development constraints and carbon neutrality targets.

Long-term monitoring and adaptive management protocols are required to track the accuracy of land-use projections and carbon storage estimates as development unfolds, enabling iterative model refinements and policy adjustments. Scalability testing with larger node networks would clarify the computational and communication overhead characteristics of federated land-use models in regions with dozens or hundreds of participating jurisdictions. Asynchronous aggregation strategies and hierarchical federation architectures may improve convergence efficiency in heterogeneous environments, where client computational capacity and network connectivity vary substantially. The integration of temporal carbon density dynamics into the InVEST module would address the current limitations in capturing forest growth, soil carbon accumulation, and climate-induced changes in ecosystem carbon stocks over multi-decadal projection periods.

The convergence of federated learning with spatially explicit ecosystem service modelling opens new pathways for privacy-preserving collaborative environmental planning in an era of increasing data sovereignty requirements and institutional fragmentation. The demonstrated feasibility of the FedProx-PLUS-InVEST framework in the Batticaloa Lagoon watershed provides a foundation for extending privacy-preserving distributed machine learning to other domains of regional environmental assessment, including coastal zone management, watershed planning, and biodiversity conservation prioritisation in the future. As multi-jurisdictional coordination becomes increasingly critical for addressing landscape-scale environmental challenges, federated learning offers a technical solution that reconciles the competing imperatives of collaborative modelling and data sovereignty, enabling evidence-based regional planning without requiring centralised data aggregation.

Statement of the Use of Generative AI and AI-Assisted Technologies in the Writing Process

During the preparation of this manuscript, the authors used QuillBot and Paper pal for language editing and refinement of the sentence structure. After using this tool, the authors reviewed and edited the content as needed and took full responsibility for the content of the published articles.

Author Contributions

Conceptualization: K.P.; Methodology: K.P.; Software: K.P. and H.S.P.; Formal Analysis: K.P. and H.S.P. All authors have read and agreed to the published version of the manuscript.

Ethics Statement

This study did not involve human subjects, animal experiments, or the collection of primary data requiring ethical approval. All geospatial data used were obtained from publicly available sources and derived from remote sensing imagery. This research complies with all relevant ethical guidelines for environmental and geospatial research.

Informed Consent Statement

“Not applicable” for studies not involving humans

Data Availability Statement

Land use data, carbon density parameters, and model outputs supporting the findings of this study are available from the corresponding author upon reasonable request.

Funding

This research received no external funding.

Declaration of Competing Interest

The authors declare that they have no known competing financial interests or personal relationships that could have appeared to influence the work reported in this paper.

References

1. Wang R, Zhao J, Lin Y, Chen G, Cao Q, Feng Y. Land Change Simulation and Forest Carbon Storage of Central Yunnan Urban Agglomeration, China Based on SSP-RCP Scenarios. *Forests* **2022**, *13*, 2030. DOI:10.3390/f13122030
2. Gu H, Li J, Wang S. Multi-Scenario Simulation of Land Use/Cover Change and Terrestrial Ecosystem Carbon Reserve Response in Liaoning Province, China. *Sustainability* **2024**, *16*, 8244. DOI:10.3390/su16188244
3. Johnson JA, Thakrar SK. Projecting global changes in land use and ecosystem services using the Spatial Economic Allocation Landscape Simulator (SEALS). *EarthArXiv* **2024**. DOI:10.31223/x5gx36
4. Wang Q, Zhang W, Xia J, Ou D, Tian Z, Gao X. Multi-Scenario Simulation of Land-Use/Land-Cover Changes and Carbon Storage Prediction Coupled with the SD-PLUS-InVEST Model: A Case Study of the Tuojiang River Basin, China. *Land* **2024**, *13*, 1518. DOI:10.3390/land13091518
5. Li M, Luo H, Qin Z, Tong Y. Spatial-Temporal Simulation of Carbon Storage Based on Land Use in Yangtze River Delta under SSP-RCP Scenarios. *Land* **2023**, *12*, 399. DOI:10.3390/land12020399
6. He Y, Ma J, Zhang C, Yang H. Spatio-Temporal Evolution and Prediction of Carbon Storage in Guilin Based on FLUS and InVEST Models. *Remote Sens.* **2023**, *15*, 1445. DOI:10.3390/rs15051445
7. Liu K, Zhang C, Zhang H, Xu H, Xia W. Spatiotemporal Variation and Dynamic Simulation of Ecosystem Carbon Storage in the Loess Plateau Based on PLUS and InVEST Models. *Land* **2023**, *12*, 1065. DOI:10.3390/land12051065
8. Jin Y, Li Y, Zhang H, Liu X, Shi H. Evaluation of Effectiveness and Multi-Scenario Analysis of Land Use Development Strategies and Ecological Protection Redlines on Carbon Storage in the Great Bay Area of China Using the PLUS-InVEST-PSM Model. *Land* **2024**, *13*, 1918. DOI:10.3390/land13111918
9. Cai J, Chi H, Lu N, Bian J, Chen H, Yu J, et al. Analysis of Spatiotemporal Predictions and Drivers of Carbon Storage in the Pearl River Delta Urban Agglomeration via the PLUS-InVEST-GeoDetector Model. *Energies* **2024**, *17*, 5093. DOI:10.3390/en17205093
10. Xing X, Wang Q, Meng F, Liu P, Huang L, Zhuo W. Assessing the Land Use-Carbon Storage Nexus Along G318: A Coupled SD-PLUS-InVEST Model Approach for Spatiotemporal Coordination Optimization. *Land* **2025**, *14*, 2067. DOI:10.3390/land14102067
11. Wang S, Li Q, Qiao L, Li F, Gao G, Lei G, et al. Coupled PLUS-InVEST Modeling of Land Use Change and the Economic Valuation of Carbon Storage in Xi'an, China. *Res. Sq.* **2025**. DOI:10.21203/rs.3.rs-7404029/v1
12. Wei X, Zhang S, Luo P, Zhang S, Wang H, Kong D, et al. A Multi-Scenario Prediction and Spatiotemporal Analysis of the Land Use and Carbon Storage Response in Shaanxi. *Remote Sens.* **2023**, *15*, 5036. DOI:10.3390/rs15205036
13. Kawnine A, Palma F, Azghadi SAR, Cao H. Encoded Spatial Attribute in Multi-Tier Federated Learning. In Proceedings of the 2025 IEEE International Conference on Consumer Electronics (ICCE), Las Vegas, NV, USA, 11–14 January 2025. DOI:10.1109/ICCE63647.2025.10929916
14. Cui L, Tang W, Zheng S, Singh RP. Ecological Protection Alone Is Not Enough to Conserve Ecosystem Carbon Storage: Evidence from Guangdong, China. *Land* **2022**, *12*, 111. DOI:10.3390/land12010111
15. Zhao H, Peng P, Chen C, Huang L, Liu G. FedRS-Bench: A Realistic Federated Learning Dataset and Benchmark for Remote Sensing. *arXiv* **2025**, arXiv:2505.08325. DOI:10.2139/ssrn.6865775
16. Li X, Li C, Yu S, Cheng L, Li D, Wang J, et al. Dynamic Simulation of Land Use Change and Assessment of Carbon Storage Based on the PLUS Model: A Case Study of the Most Livable City, Weihai, China. *Sustainability* **2024**, *16*, 10826. DOI:10.3390/su162410826
17. Nie Q, Man W, Li Z, Wu X. From Policy to Practice: Assessing Carbon Storage in Fujian Province Using Patch-Generating Land Use Simulation and Integrated Valuation of Ecosystem Services and Tradeoffs Models. *Land* **2025**, *14*, 179. DOI:10.3390/land14010179
18. Chen L, Ma Y. Exploring the Spatial and Temporal Changes of Carbon Storage in Different Development Scenarios in Foshan, China. *Forests* **2022**, *13*, 2177. DOI:10.3390/f13122177
19. Zhou J, Johnson VC, Shi J, Tan ML, Zhang F. Multi-scenario land use change simulation and spatial-temporal evolution of carbon storage in the Yangtze River Delta region based on the PLUS-InVEST model. *PLoS ONE* **2025**, *20*, e0316255. DOI:10.1371/journal.pone.0316255
20. Li L, Yu F, Junjie H, Yang Z, He Y. Spatio-Temporal Evolution of Land Use and Carbon Stock Under Multiple Scenarios Based on the PLUS-InVEST Model: A Case Study of Chengdu. *Sustainability* **2025**, *17*, 9903. DOI:10.3390/su17219903

21. Ren DF, Cao AH, Wang FY. Response and Multi-Scenario Prediction of Carbon Storage and Habitat Quality to Land Use in Liaoning Province, China. *Sustainability* **2023**, *15*, 4500. DOI:10.3390/su15054500
22. Tan J, Li Y, Bartalev SA, Stanislav S, Dang B, Zhang Y, et al. Bridging data islands: Geographic heterogeneity-aware federated learning for collaborative remote sensing semantic segmentation. *arXiv* **2024**, arXiv:2404.09292. DOI:10.48550/arXiv.2404.09292
23. Jiang Y, Ouyang B, Yan Z. The Response of Carbon Storage to Multi-Objective Land Use/Cover Spatial Optimization and Vulnerability Assessment. *Sustainability* **2024**, *16*, 2235. DOI:10.3390/su16062235
24. Madni HA, Umer RM, Foresti GL. Exploiting Data Diversity in Multi-Domain Federated Learning. *Mach. Learn. Sci. Technol.* **2024**, *5*, 2. DOI:10.1088/2632-2153/ad4768
25. Zhang R, Chen Y, Wu C, Wang F. Multi-Level Personalized Federated Learning on Heterogeneous and Long-Tailed Data. *IEEE Trans. Mob. Comput.* **2024**, *23*, 12396–12409. DOI:10.1109/tmc.2024.3409159
26. Mc Cutchan M, Giannopoulos I. Encoding Geospatial Vector Data for Deep Learning: LULC as a Use Case. *Remote Sens.* **2022**, *14*, 2812. DOI:10.3390/rs14122812
27. Gao J, Li Y, Ahmed SF. Fed-LDR: Federated Local Data-infused Graph Creation with Node-centric Model Refinement. In Proceedings of the 2024 IEEE International Conference on Data Mining Workshops (ICDMW), Abu Dhabi, United Arab Emirates, 9 December 2024. DOI:10.1109/ICDMW65004.2024.00105
28. Shi J, Abdulah S, Sun Y, Genton MG. Scalable asynchronous federated modelling of spatial data. *arXiv* **2025**, arXiv:2510.01771. DOI:10.48550/arXiv.2510.01771
29. Kanagavelu R, Garai P, Dua K, Elias S, Thomas N, Elias S, et al. Fedukd: Federated Unet Model with Knowledge Distillation for Land Use Classificationfrom Satellite and Street Views. *Soc. Sci. Res. Netw.* **2022**. DOI:10.2139/ssrn.4062814
30. Jockusch O, Hossain MZ, Imteaj A, Shahid AR. Generative AI-based Land Cover Classification via Federated Learning CNNs: Sustainable Insights from UAV Imagery. In Proceedings of the 2024 IEEE Conference on Technologies for Sustainability (SusTech), Portland, OR, USA, 14–17 April 2024. DOI:10.1109/SusTech60925.2024.10553449
31. Chen J, Zhang X, Wang K, Yan Z, Zhang W, Niu L, et al. Spatial-Temporal Evolution and Prediction of Carbon Storage in Areas Rich in Ancient Remains: A Case Study of the Zhouyuan Region, China. *Land* **2023**, *12*, 1266. DOI:10.3390/land12061266
32. Zhang Q, Huang R, Zhu C, Huang L, Yang D. Integrating land use simulation and carbon assessment for sustainable urban planning in Fuzhou metropolitan area using PLUS and InVEST models. *Sci. Rep.* **2025**, *15*, 28421. DOI:10.1038/s41598-025-13961-w
33. Partheepan K, Musthafa MM, Bhavan T, Murgante B. Harmonizing ecosystem services assessments with sustainable development goals: A case study of the Batticaloa Lagoon Watershed, Sri Lanka. *City Territ. Archit.* **2025**, *12*, 26. DOI:10.1186/s40410-025-00275-7
34. Wu L, Du J, Liu X, Li L, Zhu X, Chen X, et al. Comparative Analysis of Carbon Density Simulation Methods in Grassland Ecosystems: A Case Study from Gansu Province, China. *Remote Sens.* **2025**, *17*, 172. DOI:10.3390/rs17010172
35. Huang B, Zhang L, Wu B. Spatiotemporal analysis of rural-urban land conversion. *Int. J. Geogr. Inf. Sci.* **2009**, *23*, 379–398. DOI:10.1080/13658810802119685
36. Rimal B, Sharma R, Kunwar R, Keshtkar H, Stork NE, Rijal S, et al. Effects of land use and land cover change on ecosystem services in the Koshi River Basin, Eastern Nepal. *Ecosyst. Serv.* **2019**, *38*, 100963. DOI:10.1016/j.ecoser.2019.100963
37. Potapov P, Hansen MC, Pickens A, Hernandez-Serna A, Tyukavina A, Turubanova S, et al. The Global 2000–2020 Land Cover and Land Use Change Dataset Derived From the Landsat Archive: First Results. *Front. Remote Sens.* **2022**, *3*, 856903. DOI:10.3389/frsen.2022.856903
38. Abbasi A, Dong F, Wang X, Leung H, Zhou J, Drew S. FedGreen: Carbon-Aware Federated Learning with Model Size Adaptation. In Proceedings of the 2024 IEEE International Conference on Communications Workshops (ICC Workshops), Denver, CO, USA, 9–13 June 2024. DOI:10.1109/ICCWorkshops59551.2024.10615720
39. Guerra A, Resende F, Bergier I, Fairbrass A, Bernardino C, Centurião DAS, et al. Land use and regulating ecosystem services scenarios for the Brazilian Pantanal and its surroundings under different storylines of future regional development. *Conserv. Sci. Pract.* **2025**, *7*, e70012. DOI:10.1111/csp2.70012
40. Gong W, Duan X, Mao M, Hu J, Sun Y, Wu G, et al. Assessing the impact of land use and changes in land cover related to carbon storage by linking trajectory analysis and InVEST models in the Nandu River Basin on Hainan Island in China. *Front. Environ. Sci.* **2022**, *10*, 1038752. DOI:10.3389/fenvs.2022.1038752
41. Borthakur A, Srivastava A, Kasliwal A, Sheet D. Fed2Tier: A Two-Tier Federated Learning System Towards Green Computation. In Proceedings of the Third International Conference on AI-ML Systems, Bangalore, India, 25–28 October 2023; pp. 1–3. DOI:10.1145/3639856.3639909

42. Richards Arputharaj D, Rodriguez C, Rodio A, Neglia G. Green federated learning via carbon-aware client and time slot scheduling. *arXiv* **2025**, arXiv:2509.08980. DOI:10.48550/arXiv.2509.08980
43. Arjun T, Prashanth K, Lekshmi RC. Multimodal federated learning for privacy-preserving urban carbon footprint prediction: A framework for sustainable smart cities. In Proceedings of the 2025 International Conference on Power, Instrumentation, Control, and Computing (PICC), Thrissur, India, 9–11 October 2025
44. Polato M, Hammer BE, Roder M, Schleif F-M. Learning in federated and dynamic environments: A tutorial on challenges, trends, and practical strategies. *Neurocomputing* **2026**, *672*, 132671. DOI:10.1016/j.neucom.2026.132671
45. Yang Z, Chen M, Saad W, Hong CS, Shikh-Bahaei M. Energy Efficient Federated Learning Over Wireless Communication Networks. *IEEE Trans. Wirel. Commun.* **2021**, *20*, 1935–1949. DOI:10.1109/TWC.2020.3037554
46. Abhisha K, Abel Jopaul VP. Federated learning for privacy-preserving climate data analysis: Enabling collaborative insights without data sharing. *Int. J. Emerg. Trends Eng. Dev.* **2025**, *15*, 188–195. DOI:10.5281/zenodo.17475669
47. Wang C, Li M, Wang X, Deng M, Wu Y, Hong W. Spatio-Temporal Dynamics of Carbon Storage in Rapidly Urbanizing Shenzhen, China: Insights and Predictions. *Land* **2024**, *13*, 1566. DOI:10.3390/land13101566
48. Qu Y, Rao J, Gao S, Zhang Q, Chao WL, Su Y, et al. FLEE-GNN: A federated learning system for edge-enhanced graph neural network in analysing geospatial resilience of multicommodity food flows. In Proceedings of the 6th ACM SIGSPATIAL International Workshop on AI for Geographic Knowledge Discovery, Hamburg, Germany, 13 November 2023. DOI:10.1145/3615886.3627742
49. Wang C, Li T, Guo X, Xia L, Lu C, Wang C. Plus-InVEST Study of the Chengdu-Chongqing Urban Agglomeration's Land-Use Change and Carbon Storage. *Land* **2022**, *11*, 1617. DOI:10.3390/land11101617
50. Kang J, Zhang B, Dang A. A novel geospatial machine learning approach to quantify non-linear effects of land use/land cover change (LULCC) on carbon dynamics. *Int. J. Appl. Earth Obs. Geoinf.* **2024**, *128*, 103712. DOI:10.1016/j.jag.2024.103712
51. Kulasegaram P, Musthafa MM, Bhavan T, Murgante B. Bridging the divide: Reconciling stakeholder values for payment for ecosystem services. *TeMA J. Land Use Mobil. Environ.* **2025**, *18*, 47–66. DOI:10.6093/1970-9870/12627